Universidade de Aveiro

2019

Departamento de Ciências Médicas

DANIELA CLAUDINO CARVOEIRO

MODULATING IMMUNE RESPONSES BY TARGETING PROTEIN AGGREGATION

Modulação da Resposta Imunológica Através da Manipulação de Agregados Proteicos

Universidade de Aveiro

2019

Departamento de Ciências Médicas

DANIELA CLAUDINO CARVOEIRO

MODULAÇÃO DA RESPOSTA IMUNOLÓGICA ATRAVÉS DA MANIPULAÇÃO DE AGREGADOS PROTEICOS

Modulating Immune Responses by Targeting Protein Aggregation

Dissertação apresentada à Universidade de Aveiro para cumprimento dos requisitos necessários à obtenção do grau de Mestre em Biomedicina Molecular, realizada sob a orientação científica da Dr. Catarina Rodrigues de Almeida, Professora Auxiliar do Departamento de Ciências Médica da Universidade de Aveiro

Esta tese teve o apoio financeiro de fundos FEDER, através do Programa Operacional Competitividade e Internacionalização (POCI) – COMPETE 2020 por fundos nacionais através da FCT – Fundação para a Ciência e a Tecnologia no âmbito dos projetos StressIn (PTDC/IMI-IMU/3615/2014 e POCI-01-0145-FEDER-016768), IDPhagy (PTDC/BIA-CEL/28791/2017 e POCI-01-0145-FEDER-028791) e o projeto do iBiMED (UID/BIM/04501/2019 e POCI-01-0145-FEDER-007628).

o júri

Presidente	Professor Doutor Bruno Miguel Bernardes de Jesus Professor Auxiliar em Regime Laboral, Universidade de Aveiro
Arguente	Doutor Duarte Custal Ferreira Barral Investigador Principal CEDOC, NOVA Medical School | Faculdade de Ciências Médicas Universidade NOVA de Lisboa
Orientadora	Professora Doutora Catarina Rodrigues de Almeida Professora Auxiliar em Regime Laboral, Universidade de Aveiro

Agradecimentos

Ao finalizar esta dissertação de mestrado não posso deixar de agradecer:

À minha orientadora, Professora Doutora Catarina Almeida, pela supervisão, pelo apoio constante, pelos ensinamentos transmitidos e acima de tudo pela oportunidade de trabalhar com a sua fantástica equipa onde aprendi tanto. Estarei eternamente grata.

Ao Paulo Antas, pela amizade, constante dedicação, paciência e disponibilidade. Por todos os ensinamentos. Um especial agradecimento por toda a ajuda e pela grande influência na vida profissional.

À equipa de Immune Cell Biology do iBiMED, por todo o apoio, ajuda e ensinamentos ao longo deste ano. Obrigado por me ensinarem o que é bom trabalho de equipa. Foi um prazer trabalhar com todos vocês.

Aos meus pais, Natércia e Luís, e a minha irmã, Marisa, pela paciência, compreensão e apoio incondicional. Obrigado por todos os sacrifícios. A vocês devo quem sou hoje.

À Rute Ribeiro e ao João Aparício por me ensinarem que família é muito mais que uma percentagem de DNA em comum.

À Bárbara Andrade, à Joana Dias, à Margarida Vaz, e à Tatiana Magro pela amizade e apoio ao longo destes últimos dois anos.

À minha Família Virgínia, por me mostrarem que a amizade consegue vencer a distância: Anabela Santos, Carolina Silva, Diana Dantas, Márcia Braz, Margarida Vaz e Mariana Gomes.

palavras-chave

pDC, resposta inflamatória, agregados proteicos, DALIS, proteossoma, p62, inflamassoma.

resumo

A agregação de proteínas é um processo que pode ser induzido por uma grande variedade de stresses celulares, incluindo privação de aminoácidos, infeção viral, stress do retículo endoplasmático, lipopolissacarídeos, e stress oxidativo. Alterações na proteostase parecem ter um impacto na resposta inflamatória, mas os mecanismos subjacentes a este impacto são ainda pouco conhecidos. Esta tese tem por objetivo analisar de que forma a agregação de proteínas influencia a resposta das células dendríticas humanas, em particular das células dendríticas plasmocitóides (pDCs). Foram utilizados inibidores de autofagia e do proteossoma para manipular o número de agregados na linha celular de pDCs, CAL-1. A inibição do proteossoma em pDCs induziu a formação de agregados constituídos por p62 de grandes dimensões, e levou à secreção de IL-1β e morte celular, de forma irreversível e específica destas células. Os mesmos efeitos não foram observados após inibição da autofagia nem se verificaram numa outra linha celular, monocítica. Para estudar o mecanismo por detrás do aumento da resposta inflamatória após a inibição do proteossoma, foram criadas células knockout para o p62 usando o sistema CRISPR/Cas9. Os nossos resultados sugerem que nem o p62 nem o inflamassoma de NLRP3 são necessários para a indução da morte celular por inibição do proteossoma em pDCs. De forma geral, concluímos que a inibição do proteossoma induz uma resposta inflamatória específica para pDCs. Propomos que esse efeito deve ser tido em consideração quando se utilizem inibidores de proteossoma como potenciais fármacos para o tratamento de distúrbios mediados por pDCs e, portanto, mais estudos devem ser feitos para esclarecer o efeito da inibição do proteossoma em pDCs.

keywords pDC, inflammatory response, protein aggregates, DALIS, proteasome, p62, inflammasome.

abstract

Protein aggregation is induced by a wide variety of cellular stresses, including amino acid starvation, virus infection, endoplasmic reticulum stress, lipopolysaccharide, and oxidative stress. It has been suggested that altered proteostasis impacts the inflammatory response, but the underlying mechanism between altered proteostasis and inflammation is still poorly understood. Here, we aim to analyse the impact of protein aggregation in the response of human Dendritic Cells, focusing on plasmacytoid dendritic cells (pDCs). The number of aggregates was manipulated in a pDC cell line, CAL-1, by using both autophagy and proteasome inhibitors. Proteasome inhibition in pDCs induced assembly of large p62-based aggregates, together with an increase on IL-1β secretion and cell death, in an irreversible and cell specific manner. The same effects were not observed upon autophagy inhibition nor on a monocytic cell line. To study the mechanism behind the increase in the inflammatory response upon proteasome inhibition, p62-knockout cells were generated using the CRISPR/Cas9 system. Our data suggests that neither p62 nor the NLRP3 inflammasome are required for induction of cell death upon proteasome inhibition in pDCs. Overall, we conclude that proteasome inhibition induces an inflammatory response specific to pDCs. We propose that this effect must be considered when using proteasome inhibitors as potential drugs for the treatment of pDCs derived immune-mediated disorder and thus, mores studies should be done to clarify the outcome of proteasome inhibition on pDCs.

Table of content

List of Figures

List of Tables

List of Abbreviations

ALIS	Aggresome-Like induced Structures
APC	Antigen-presenting cell
APS	Ammonium Persulfate
ASC	Apoptosis-associated speck-like protein containing caspase-recruitment domain
ATG	Autophagy-related protein
BCA	Bicinchoninic Acid
BSA	Bovine Serum Albumin
CARD	Caspase Recruitment Domain
CP	constitutive Core Particle
cDC	Conventional Dendritic Dell
DALIS	Dendritic cell Aggresome-Like induced Structures
DAMP	Danger-Associated Molecular Patter
DC	Dendritic Cell
DRiPs	Defective Ribosomal Products
ER	Endoplasmic Reticulum
FBS	Fetal Bovine Serum
FDA	Food and Drug Administratio
GFP	Green Fluorescent Protein
GVHD	Graft-Versus-Host Disease

HDAC6	Histone Deacetylase 6
iCP	Immunoproteasome Core Particle
IFN	Interferon
IL-1	Interleukin-1
IL-2	Interleukin-2
IL-4	Interleukin-4
IL-6	Interleukin-6
IL-12	Interleukin-12
IL-18	Interleukin-18
KO	Knockout
LDH	Lactate dehydrogenase
LPS	Lipopolysaccharide
mDC	Myeloid dendritic cell
MEF	Mouse Embryonic Fibroblasts
MHC-I	Major histocompatibility complex class I
MHC-II	Major histocompatibility complex class II
NEAA	Non-essential amino acids
NK	Natural Killer
NLR	NOD-like receptor
PAMP	Pathogen-Associated Molecular Patter
PBS	Phosphate-buffered saline

PCR	Polymerase Chain Reaction
pDC	Plasmacytoid Dendritic Cell
RIG	Retinoic Acid Inducible Gene
RLR	RIG-I-like Receptors
ROS	Reactive Oxygen Species
RP	Regulatory Particle
SDS	Sodium dodecyl sulfate
SING	Stimulator of interferon genes
SOCS1	Suppressor of cytokine signaling 1
TBS	Tris-buffered saline
tCP	Thymoproteasome Core Particle
TLR	Toll-like-receptor
TNF	Tumor necrosis factor
UPS	Ubiquitin-proteasome system
PVDF	Polyvinylidene Difluoride

1. Introduction

The immune response is triggered when an individual's immune system recognizes antigenic foreign substances (both non-self and altered self) and responds by excluding these substances that threaten normal homeostasis. Fundamental to the immune system's capacity to mobilize a response to an invading pathogen or toxin is its ability to distinguish self from non-self (1). This ability is essential to avoid responses that produce excessive damage against self-tissues or that might eliminate beneficial, commensal microbes. Failure to modulate the inflammatory response underlies the broad class of autoimmune and autoinflammatory diseases, therefore, it is of great importance to understand what influences and modulates the immune response (1,2). The immune system relies on a complex array of protective mechanisms to modulate its response (1). Within these protective mechanisms, proteostasis has been increasingly recognized to have a role in the immune response, and altered proteostasis has been associated with auto-inflammatory disorders (2,3). A disruption in the protein homeostatic machinery, such as that of autophagy or the ubiquitin-proteasome pathway, can induce an accumulation of misfolded proteins, resulting in altered proteostasis (3,4). It has been suggested that altered proteostasis results in inflammasome activation in macrophages, but the underlying mechanism between altered proteostasis and inflammatory disorders is still poorly understood (4). Dendritic Cells (DCs) are best known for their potent ability to initiate adaptive immunity, being versatile and essential controllers of the immune system (5). With that in mind, we attempted to understand how altered proteostasis influences the function of DCs.

1.1. Dendritic cells

Dendritic cells are professional antigen-presenting cells (APCs) that are responsible for initiation of adaptive immune responses, due to their remarkably strong capacity to present antigens to both naïve CD4 and CD8 T lymphocytes and secrete cytokines that regulate subsequent responses (6,7). In their immature state, most DCs migrate to peripheral organs where they detect and capture incoming pathogens. Detection by organ-resident DCs of pathogen- and/or danger-associated molecular patterns (PAMPS and/or DAMPs) rapidly activates different metabolic, cellular and gene expression programs that induce their maturation and migration towards the lymph nodes (8). DCs can take up a diverse array of

antigens and present them to T cells as peptides bound to both major histocompatibility complex class I (MHC-I) and MHC-II proteins. Conversely, DCs can capture proteins in the stable state, i.e., in the absence of microbial or other perturbations, allowing them to control tolerance to self and "normal" environmental constituents by presenting self-antigens to and anergizing autoreactive T cells (6). In addition to their role in initiating adaptive responses, DCs also play an important role in innate immunity. DCs can produce copious amounts of cytokines involved in the host's defence against a microbial pathogen, such as interleukin-2 (IL-2) and both type I and II interferons. Furthermore, DCs can activate natural killer (NK) and NKT cells, innate lymphocytes that rapidly kill selected targets and produce important cytokines (6). DCs are, therefore, vital regulators of the immune system, and their maturation process reflects an ordered series of signal-dependent events resulting in specific and dramatic phenotypic and functional changes, leading to powerful immunomodulatory functions (6). Furthermore, there are different subsets of DCs that are endowed with different characteristics and lead to different types of immune responses. Two major DC subtypes have been identified in humans, the myeloid/conventional DCs (mDCs or cDCs) and the plasmacytoid DCs (pDCs) (9,10).

1.1.1. Plasmacytoid dendritic cells

Plasmacytoid dendritic cells are a subpopulation of DCs with the remarkable capacity to rapidly produce copious amounts of type I interferon (IFN-I) when stimulated by nucleic acids that bind and activate toll-like-receptor (TLR)9 or TLR7 (11). pDCs are rare cells that develop in the bone marrow and circulate within the blood compartment and lymphoid organs (12). The circulation of pDC can be compared with lymphocytes and their antigen processing and the regulation of their MHC-II expression resemble that of B cells rather than cDCs (13). They have the morphology of an antibody-secreting cell and play a critical role as part of the first line of defence against various infections, primary viral infections (11). This type of cells also links the innate and adaptive immunity since they induce the migration of NK cells, maturation of other DCs and macrophages, antigen presentation, T cell response and differentiation of antibody-producing plasma cells (14,15).

Upon activation of TLR9 or TLR7, within endosomal compartments, by nucleic acids derived from viruses, bacteria, or dead cells, pDC respond rapidly with abundant IFN α/β secretion, which can be up to 1.000-fold more potent than in other cell types (16). In addition to IFN-I production, TLR induced pDC activation has added consequences, including the secretion of pro-inflammatory cytokines and chemokines, such as IL-6, IL-12, TNF-α, and the acquisition of antigen presentation ability (14,15). Depending on the environment and

the type of stimulation, pDCs can participate in the priming of either immunogenic or tolerogenic adaptive immune responses (17). The expression of MHC and T cell costimulatory molecules in activated pDCs is not as high as on cDCs, but, nevertheless, pDCs can stimulate immunity or sustain protective responses at sites of infection. On the other hand, pDCs can induce T cell tolerance primarily through the induction of regulatory T cells, a characteristic they also share with cDCs (17) .

1.2. Accumulation of protein aggregates in dendritic cells

When bone-marrow-derived cDC from mice are activated by PAMPs, DAMPs or fever-like temperature, large poly-ubiquitinated protein aggregates, named dendritic cell Aggresome-Like Induced Structures (DALIS), are formed (18,19). DALIS are structures that resemble the aggresome since both DALIS and aggresomes contain ubiquitinated proteins. The aggresome is a pericentriolar cytoprotective structure formed by microtubule-dependent conglomeration of smaller aggregates and redistribution of the intermediate filament protein vimentin, to deal with the increasing demand for clearance of misfolded/aggregated proteins (20). However, unlike classical aggresomes, DALIS do not localize in the pericentriolar area of the cell, they also are not caged with vimentin and are not sensitive to microtubule or actin cytoskeletal disruptors (18). Moreover, DALIS are transient in nature and can be detected in bone-marrow-derived cDC, from mice, as soon as 4h after TLR4 activation by a lipopolysaccharide (LPS) and dissipate 20-44h later (18,21). DALIS formation and maintenance has been linked to the rapid increase of protein synthesis activity occurring upon TLR triggering, suggesting that most of the molecular material incorporated in the aggregates are made of ubiquitinated newly synthesized proteins (22,23). Ubiquitin is a small regulatory protein involved in many cellular functions, including ribosome biosynthesis, gene expression, receptor expression, stress response and protein degradation by 26S proteasomes (24,25). Nevertheless, DALIS formation does not affect the ubiquitin-proteasome pathway and is not due to impaired proteolysis (18).

DALIS are thought to contain defective ribosomal products (DRiPs), which can account for up to 30% of newly synthesized protein, that, due to the errors in their synthesis, are rapidly ubiquitinated and degraded (18,26). It has been proposed that DRiPs are a major source of self- or viral antigenic peptides for MHC-I restricted presentation (26–28). Typically, DRiPs are quickly degraded by proteasomes; However, ubiquitinated proteins contained in DALIS have a much longer half-life than those present in the cytosol, delaying their degradation and stabilizing them for 8-16h (23). Another study suggests that DRiPs

are either selectively degraded by autophagy or by the proteasome and that it can occur some degree of communication between the two degradation pathways (29). Given that the peak of antigen presentation by MHC-I takes place several hours after DC activation, maturing DCs might have the ability to delay MHC-I loading and peptide presentation until the secretion of proinflammatory cytokines and the expression of costimulatory molecules has been initiated by delaying the degradation of newly synthesized misfolded protein through the formation of DALIS (21,23,26,30). Therefore, DALIS represent dynamic repositories for poly-ubiquitinated newly synthesized DRiPs (18,23).

The immune context appears to also play a role in DALIS accumulation, as different cytokines can lead to either inhibition or induction of DALIS formation (31,32). For instance, mouse bone-marrow-derived cDC differentiated with IL-4 - a pleiotropic cytokine whose most important role is to support the differentiation and function of Th2 and B cells - promotes autophagy and prevents DALIS formation (31). On the other hand, IFNα, an anti-viral cytokine, seems to favour formation of DALIS in maturing human DCs (32). Overall, even though the function(s) of DALIS is still not entirely understood, their appearance in response to TLR stimulation suggests a role in the innate or adaptive immune response mounted to control infection.

Recently, it was shown that, contrary to what was previously thought, equivalent structures to DALIS, Aggresome-Like Induced Structures (ALIS), can be detected in macrophages (21) and non-immune cells upon oxidative stress or in response to different pharmacological treatments affecting protein folding and protein degradation (33). Together, these studies indicate that ALIS mediate the storage of proteins degraded by the proteasome and by autophagy in different cell types.

1.3. Autophagy

Macroautophagy (referred herein as autophagy), which is autophagy in its strictest form, refers to an intracellular degradation system by which cytoplasmic constituents are delivered to the lysosome dependently on specialized autophagy-related proteins (34). These specialized proteins promote the genesis of autophagosomes, which are double membrane organelles, that will engulf target portions of the cytoplasm and fuse to the lysosome, leading to final degradation of its content by lysosomal degradation enzymes (8). When induced at low frequency, under steady-state conditions, autophagy contributes to cellular homeostasis as it promotes the turnover of organelles, such as damaged

mitochondria, and avoids the accumulation of protein aggregates (35). Autophagy is induced both under nutrient-starvation, contributing to the reuse of cytoplasmic constituents, including amino acids and lipids, and in order to eliminate unfavourable intracellular constituents such as invading microorganisms (35).

1.3.1. Autophagy and assembly of Dendritic Cell Aggresome-Like-Induced Structure

The term aggrephagy is a type of macroautophagy and is described by the selective sequestration of protein aggregates by autophagy (36). Thus, aggrephagy plays a role in ALIS clearance. There is evidence that autophagy plays an important role in regulating (D)ALIS accumulation. A causative link between (D)ALIS formation and autophagy flux reduction was revealed when inhibition of autophagy on HeLa cells promoted accumulation of poly-ubiquitinated DRiPs together with the autophagosomal adapters NBR1 (neighbour of BRCA1 gene 1), p62 (sequestrosome 1/SQTM1), autophagy-linked FYVE protein (ALFY) proteins, and LC3/ATG8 (29,31). It was also shown that NBR1 promotes DRiPs targeting to autophagosome, whereas p62 is only essential for aggregation but not DRiPs targeting to autophagosome (29). Furthermore, p62, alongside with the histone deacetylase 6 (HDAC6), is an important determinant of aggregated localization of MyD88 – an essential adaptor molecule for TLRs and IL-1 receptor. After recruitment of p62 and HDAC6, MyD88 activates a machinery of polyubiquitinated protein accumulation to form protein aggregates, which ultimately leads to lysosomal degradation by autophagy (37). The role of autophagy inhibition for (D)ALIS formation was further confirmed by silencing *Atg5*, an essential autophagy gene (29). Furthermore, inhibiting autophagy enhances the formation of ALIS in both macrophages exposed to LPS, in the catalase inhibitor 3-amino-1,2,4-triazole (ATZ; causes oxidative stress) treated HeLa cells and in starved MEF cells (33). In the same study it was shown that inhibiting autophagy also reduced the clearance rate of puromycin-induced ALIS in HeLa cells. These results indicate that autophagy is involved in the regulation of ALIS accumulation in both immune and non-immune cells by reducing the clearance rate of these aggresome-like structure, after their formation (33). Overall, both immune and non-immune cells appear to employ autophagy to regulate (D)ALIS clearance.

1.3.2. Autophagy and the immune response

Antigen presentation by MHC proteins is essential for adaptive immunity. MHC-I-restricted antigens originate predominantly from endogenous newly synthesized proteins and are presented to primed CD8+ cytotoxic T lymphocytes, which can kill target cells. On

the other hand, MHC-II-restricted antigens originate mostly from extracellular proteins and are presented to CD4+ T cells, leading to the coordination and regulation of effector cells (38). Autophagy is involved in antigen presentation by MHC-II (39). This form of antigen presentation involves the degradation of endocytosed material in endo-lysosomal compartments, binding of the resulting peptides to MHC-II and activation of the MHC-II presentation machine in DC and macrophages (40). It is also involved in processing for MHC-II presentation of endogenous protein, in a process that has been named type 2 cross presentation (38). On the other hand, presentation of peptides on MHC-I derived from exogenous proteins that have been internalized by endocytosis or phagocytosis, is regulated by type 1 cross-presentation. Through this pathway, antigens captured from the extracellular environment are degraded in the cytosol by the proteasome and the resulting peptides are transported to the endoplasmic reticulum for binding to MHC-I. The existence of these two major degradation pathways for cytosolic proteins provides professional APCs the ability to present antigens which are normally presented by MHC-II on the surface of DCs, to also be presented through the MHC-I pathway, that is antigens derived from the same exogenous protein can be presented on both MHC-I and MHC-II (8). Type 1 cross-presentation is an essential mechanism carried out primarily by specific DCs, to efficiently present exogenous antigens to $CD8^+$ T cells (41), while type 2 cross presentation is relevant for stimulation of CD4+ T cells, being important for negative T cell selection in the thymus, as well as for induction of an efficient antiviral immune response (38).

The autophagic capture of intracellular microbes and their consequent elimination via autolysosomes is the most direct way in which autophagy influences inflammation (42). The autophagic machinery enhances the delivery of viral nucleic acids to the endosomal TLR7, which activates IFN-I production and enables recognition of cytoplasmic viral replication intermediates by pDCs (42). By contrast, autophagy proteins negatively regulate the assembly of pro-inflammatory protein complexes (43–45). In autophagy deficient cells, accumulation of p62 activates the pro-inflammatory transcription factor NF-κB through a mechanism involving TRAF6 oligomerization (46). Also, it has been reported that autophagy inhibits reactive oxygen species (ROS) production by decreasing the mitochondrial mass and eliminating leaky mitochondria and peroxisomes (47). ROS trigger amplification of RIG (retinoic acid inducible gene)-I-like receptors (RLRs) – a receptor responsible for single-stranded RNA viruses' recognition - signalling, driving the production of more IFN and interleukins. Moreover, the ATG5-ATG12 complex, essential for autophagosome formation, inhibits RLR signalling by directly binding to caspase recruitment domains (CARDs) of RIG-I and IFN-β promoter stimulator protein 1 (44). Therefore, the absence of autophagy

amplifies the production of IFN-I (43). Finally, the autophagy protein ATG9A negatively controls trafficking of STING, a transmembrane protein that is essential for efficient activation of IFN-I and pro-inflammatory cytokine production in response to double-stranded DNA (45). Collectively, these data suggest the presence of a feedback loop by which autophagy downregulates IFN-I responses succeeding a period of productive induction. This feedback loop could also have the purpose of increasing the threshold for activation of IFN-I signalling (48).

In addition to regulating inflammatory signalling, autophagy may also prevent inflammation through its role in apoptotic corpse clearance. Even though autophagic death of immune competent cells could compromise defence against infection, it might also be beneficial in controlling the level and duration of inflammation. The efficient clearance of apoptotic corpses, through autophagy, prevents secondary necrosis, which would release danger signals (DAMPs) that trigger inflammation (49).

Another important effect of the autophagy pathway on the inflammatory response is related to regulation of the inflammasome-dependent responses. In this case, autophagy acts like a negative regulator of inflammasomes (50–53).

1.4. Inflammasome

Inflammasomes are intracellular signalling platforms that can sense sterile stressors such as aggregates of uric acid, ROS, and others, and that activate the pro-inflammatory cytokines interleukin-1β (IL-1β) and IL-18. These cytosolic multiprotein complexes consist of three partners: a sensor protein which recruits and activates caspase-1 in response to intracellular danger signals, the adapter protein apoptosis-associated speck-like protein containing caspase-recruitment domain (ASC), and the proinflammatory caspase, caspase-1 (54). Inflammasome assembly can be triggered by sensing a variety of stimuli that are associated with infection or cellular stress that can activate the sensor protein, generating oligomerization and recruitment of ASC, and induce activation of caspase-1. Active caspase-1 subsequently processes and releases mature IL-1α, IL-1β and IL-18. These cytokines establish a host defence line against pathogens by inducing inflammation and promoting adaptive immune responses (35). In addition to cytokine secretion, inflammasome activation can also trigger pyroptosis, a rapid and highly pro-inflammatory form of programmed cell death, which serves to blunt intracellular pathogen replication (55).

The NOD-like receptor (NLR) family was the first family of sensor proteins discovered to form inflammasomes and is comprised of 22 human genes. Currently, the NLRP3 inflammasome is the most thoroughly studied and characterized inflammasome and consists of the NLRP3 scaffold, the ASC (PYCARD) adaptor, and caspase-1. NLRP3 is activated upon exposure to a diverse set of microbes, which includes viral, bacterial, fungal, and protozoan pathogens, as well as a number of structurally diverse PAMPs, DAMPs, and environmental irritants (35). It has been described that NLRP3 inflammasome activation in response to the accumulation of various DAMPS, during the aging process, induces systemic chronic inflammation (56). NLRP3 inflammasome activation depends on priming and activation, two functionally distinct steps (54). The “priming” step licenses the cell and is provided by inflammatory stimuli, such as TLR4 agonists, resulting in the rapid activation of NF-κB, which stimulates pro-IL-1β synthesis, and increased expression of NLRP3 (54). The “activation” step is less clear; it occurs following the recognition of an NLRP3 activator, such as PAMPs and DAMPs, thereby promoting NLRP3 inflammasome assembly and caspase-1 mediated IL-1β and IL-18 secretion and pyroptosis (57).

Inflammasome proteins are expressed most prominently by macrophages and DCs (58). The relationship between inflammasome and DCs varies depending on the cells state; in danger/infectious scenarios NLR activation synergizes with TLR-derived pathways to expand DCs maturation and migration, antigen presentation and pro-inflammatory cytokine production, which can shape the type of T cell response (59). However, in the absence of danger signals and without TLR engagement, inflammasome activation has an immunosuppressive effect in DCs by inducing apoptosis, leading to decreased antigen presentation and driving the immunosuppressive effect of TGF-β receptor signalling (59). Regarding pDCs, it was recently shown that inactivation of inflammasome signalling reduces IL-1β secretion but increases IFN-I production (60). This study showed that inflammasome activation enhances IL-1β-mediated MyD88-TRAF3-IRF3 signalling and SOCS1 upregulation. However, SOCS1 inhibits MyD88-IRF7-mediated-IFN-1 signalling in pDCs, therefore, ablation of inflammasome components reduce SOCS1 induction, leading to high levels of IFN-α/β production. Thus, inflammasome activation seems to play a role in the negative regulation of IFN-I signalling pathways, in pDCS (60).

1.4.1. Inflammasome and autophagy

The first observation regarding the effect of autophagy on inflammasome activation was that of Saitoh et al. who reported that blockade of autophagy, by genetic ablation of the autophagy regulator Atg16L1 in murine macrophages, enables LPS-dependent

inflammasome activation, suggesting that autophagy normally counters inflammasome activation by LPS (50). Align with this idea, several convergent reports support the concept that autophagy regulates inflammasome activation (51–53). As mentioned before, under sterile conditions, autophagy clears the cytoplasm from debris, protein aggregates and defective organelles that can function as endogenous inflammasome agonists. Furthermore, upon exposure to microbial infection, the autophagy pathway eliminates damaged organelles. If autophagy is blocked, this leads to an accumulation of depolarized mitochondria, that release inflammasome activators such as mitochondrial DNA and ROS (51). Thus, it has been proposed that the degradation of damaged mitochondria by autophagy prevents excess NLRP3-inflammasome activation and, therefore, excessive production of IL-1β. Moreover, it has been suggested that autophagy may downregulate prolonged inflammasome activity by removing aggregated inflammasome components (53). Aggrephagy may also play a role in inflammasome activation, since it has been suggested that altered proteostasis results in inflammasome hyperactivation in autophagy deficient primary macrophages (4). However, the mechanism underlying autophagy-dependent inflammasome inhibition is still not entirely clear.

1.5. Proteasome

The ubiquitin-proteasome system (UPS) is responsible for the degradation of approximately 80% of all cellular proteins, thus having a predominant role in homeostasis between protein synthesis and degradation in eukaryotic cells (61). Therefore, the UPS controls almost all basic cellular processes, such as cell cycle progression, DNA replication, signal transduction, cell death, stress responses, immune responses and metabolism (62,63). The proteasome, a large and tightly regulated protein complex of over 2.5 MDa, is at the heart of this eukaryotic protein degradation machinery (63). Protein destruction is initiated by attachment of a typical ubiquitination pattern for recognition by the proteasome, which comprises a chain of at least four ubiquitin molecules that act as a signal that shuttles the target protein to the proteasome, where the substrate is proteolytically broken down (63,64).

The proteasome can be found in the cytoplasm as well as the nucleus of eukaryotic cells, and is made up of two subcomplexes: a proteolytic core particle (CP), the 20S proteasome, and one or two 19S “cap” regulatory particle(s) (RP) that serves as a proteasome activator (63,65). To form an enzymatically active proteasome, the 26S proteasome, the 19S RP binds to one or both ends of the latent 20S proteasome. The 19S

RP recognizes ubiquitylated client proteins and is thought to play a role in their unfolding and translocation into the interior of the 20S CP, which progressively degrades the client proteins, generating oligopeptides, through the catalytic threonine residues contained on the surface of a chamber formed by two β-ring (Figure 1) (63). All the active sites of the proteasome are confined to the inner cavity of the 20S core, which is only reachable through the gated channel in the α-rings that are too narrow to be traversed by tightly folded proteins, thereby preventing uncontrolled destruction of the bulk of cellular proteins (65,66). Three different types of CPs have been identified, in vertebrates: the constitutive (CP), highly abundant and present in all tissues; the immunoproteasome (iCP), present predominantly in monocytes and lymphocytes; and the thymoproteasome (tCP), exclusively found in cortical thymic epithelial cells (61,67,68). The iCP and tCP have enhanced proteolytic activity and different cleavage-site preferences. Due to such modifications, the proteolytic subunits of these specific proteasomes generate substrate epitopes for the antigen presenting MHC-I receptors of the immune system at a substantially higher rate (69,70).

1.5.1. Proteasome and Dendritic Cell Aggresome-Like-Induced Structure

As previously mentioned, (D)ALIS appear to mediate the storage of proteins degraded by the proteasome, being that the polyubiquitinated proteins contained in these structures are thought to be degraded, at least in part, through the action of the proteasome (18,23); thus, proteasome inhibition could enhance DALIS accumulation in DCs. However, it has been shown that proteasome functionality is unaffected in maturing mouse bone-marrow-derived cDCs, and DALIS formation does not depend on nor seems to affect deeply the proteasome's activity (18). In support of this, another study showed that proteasome inhibition in HeLa cells, through epoxomicin treatment, did not result in a significant increase in ALIS occurrence (33).

Even though the proteasome has not been implicated in the assembly of ALIS, its activity has been linked to the clearance of DALIS in DCs (18). It seems that at the early stages of maturation of mouse bone-marrow-derived cDCs, the proteasome does not interfere with the disappearance of DALIS, while it participates actively in DALIS disappearance during late stages of maturation (18).

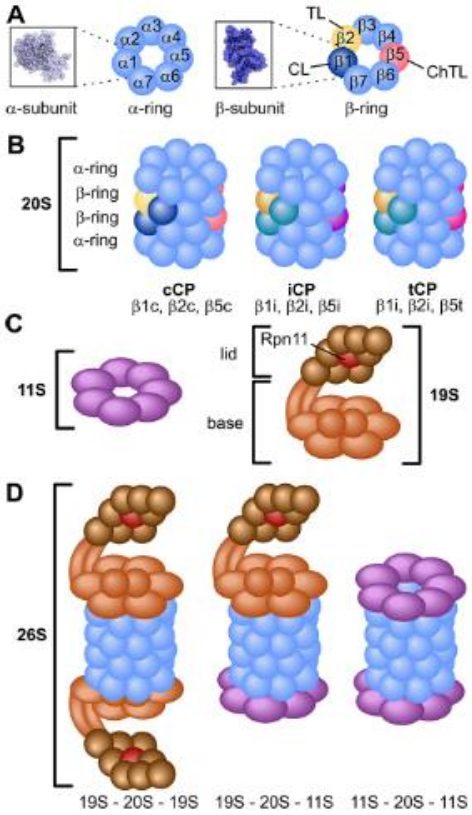

Figure 1: The proteasome. (A) α- and β-subunits are arranged in rings of seven. The catalytically active subunits are β1 (caspase-like: CL), β2 (Trypsin-like TL), and β5 (chymotrypsin-like: ChTL). **(B)** The 20S CP encompasses four rings stacked in an αββα pattern and forming the catalytic chamber. The three different 20S CPs are the cCP, iCP, and tCP and vary by their catalytic subunits. **(C)** Two proteasome lids, the 11S cap and the 19S RP. The 11S cap acts in a ubiquitin- and ATP-independent manner. The 19S RP can be divided into the base and the lid which inherits the deubiquinating enzyme Rpn11. **(D)** Different proteasome assemblies have been identified, thus far. The 26S proteasome comprises the 20S CP capped with two 19S RP. The 11S cap can either associate with the free end of a 19S−20S complex to form a hybrid proteasome or bind to both sides of the 20S CP. [adapted from (61)]

1.5.2. Proteasome inhibition

Inhibition of the proteasome can lead to various cellular outcomes, such as endoplasmic reticulum stress, NF-κB inhibition, unfolded protein response, angiogenesis inhibition, cell cycle arrest, or an accumulation of proapoptotic factors and tumour suppressors. Thus, medical interest in modulating proteasome function for therapeutic purposes has significantly increased (61,71). Studies led to FDA approval of three drugs (bortezomib, carfilzomib, and ixazomib) by demonstrating that the proteasome can be transiently and safely inhibited in humans (61). It was observed that proteasome inhibition has anti-tumour activity, especially against hematopoietic malignancies but also against solid tumours (72). The efficacy of proteasome inhibition for the treatment of cancer is based

on its role in regulating cell proliferation and on the exquisite reliance of cancer cells on proteasome function (73).

The immunoproteasome has been associated with the development and progression of neurodegenerative diseases, autoimmune disorders, inflammation, and certain types of cancer, therefore selective inhibition of immunoproteasome has gained considerable interest (70,74). Proteasome inhibition, in the immune system, results in decreased inflammatory and immune responses, with cell migration and cell adhesion being compromised, owing in part to the fundamental role of the proteasome in antigen presentation (72). Proteasome inhibition leads to T cell apoptosis, being that activated T cells are more susceptible to proteasome inhibition than resting T cells. This suggests that proteasome inhibition might be a successful strategy to treat diseases involving activated T cells, such as graft-versus-host disease (GVHD) (75). Furthermore, proteasome inhibition might be a viable strategy for the treatment of autoimmune diseases, as proteasome inhibition also results in depletion of alloreactive T cells, while the immune defence against pathogens remains intact (76).

Proteasome inhibition strongly affects DC immunogenicity by preventing the upregulation of costimulatory molecules and the increase in migratory and immunostimulatory capacity, that are usually induced by activating stimuli, such as LPS or TNF-α (77,78). Secretion of the immunostimulatory cytokines IL-12 and TNF-α upon LPS stimulation is also reduced. Furthermore, proteasome inhibition induces NF-κB activity blockage, mitochondrial re-localization and subsequent activation of the caspase cascade with consequent apoptosis (75), an effect that could be more pronounced in immature DCs (79). In addition to conventional DCs, pDCs were also recently found to be highly affected by proteasome inhibition (80). Proteasome inhibitors, such as bortezomib, inhibit intracellular trafficking of Toll-like receptors and disrupt ER homeostasis, thus impairing pDCs immunostimulatory capacity and viability (80). On the basis of this evidence, it was proposed that proteasome inhibitors may alleviate immune disorders where pDCs play a role, such as systemic lupus erythematosus.

Accumulating preclinical evidence indicates that proteasome inhibitors are strong candidates for the treatment of immune-mediated disorders. However, data is still preliminary and thus other studies must be done in order to understand the real impact of proteasome inhibition on the immune system. For instance, a study revealed that inhibition of the proteasome in DCs inhibits IL-1 degradation and leads to an accumulation of polyubiquitinated IL-1 (81). On the contrary, delayed administration of bortezomib leads to

TLR4 pathway activation and to amplified production of IL-1β and other inflammatory cytokines, which resulted in accelerated acute GVHD-dependent morbidity (82).

1.6. Objectives

(D)ALIS are transient and large cytosolic structures that contain ubiquitinated proteins and are found in DCs and macrophages upon maturation or after TLR4 activation, and whose function is still not fully understood (83). Various cellular processes, such as autophagy and UPS, interfere with (D)ALIS formation and/or clearance (18,31). The dynamic and transient profile of (D)ALIS, associated with the fact that this type of protein aggregates forms upon cell activation, leads us to believe that (D)ALIS might have a role in the inflammatory response. pDCs comprise a pivotal element of the immune response, especially regarding antiviral immune responses (84,85). Hence, understanding the mechanisms behind pDC-mediated immune response is of great importance. In that context, the primary aim of this dissertation is to dissect the role of protein aggregation on pDCs mediated inflammatory response. Taking this into account, our specific objectives are:

1. To analyse accumulation of protein aggregates in pDCs upon autophagy or proteasome inhibition;
2. To understand the consequences of either autophagy or proteasome inhibition in pDC inflammatory responses;
3. To define the role of protein aggregates in inflammation mediated by pDCs.

2. Methods:

2.1. Cell lines:

CAL-1 (a pDC line), THP-1 (a monocytic cell line) and CAL-1 $p62^{-/-}$ $GFP^{-/-}$ cells were grown in RPMI 1640 with glutamine (21875-034, Gibco), 10% heat-inactivated fetal bovine serum (FBS; F7524, Sigma), 1% Sodium Pyruvate (11369-070, Gibco), 1% HEPES (4-(2-hydroxyethyl)-1-piperazineethanesulfonic acid; 15630-056, Gibco) and 1% non-essential amino acids (NEAAs; 11140-035, Gibco), at 37ºC under a 5% CO_2 atmosphere.

2.2. Antibodies, Reagents and Drugs

Reagents were from the following suppliers: Spautin-1 (567569) from Calbiochem; MG132 (BML-PI102-0005) from Enzo Life Sciences; DAPI (D1306) and CyQUANT™ LDH Cytotoxicity Assay Kit (C20300) from Invitrogen; ProLong™ Gold Antifade Mountant (P10144), Pierce™ BCA Protein Assay Kit (23225), Pierce™ protease inhibitor mini tablets (88665), AmpliTaq Gold 360 Master mix (4398881), and Pierce™ ECL Western Blotting Substrate (32106) from ThermoFisher Scientific; ATP (A6419-1G), Sodium orthovanadate (S6508), Sodium fluoride (NaF; S6776), Doxycycline hyclate (D9891-1G), Triton™X-100 (T8787), SDS (L3771), TEMED (T9281), alcian blue 8GX (A5268), sodium azide (71289), Trypan blue solution (T8154) and LPS (L6529) from Sigma-Aldrich; MCC950 (inh-mcc) from Invivogen; Sodium chloride (NaCl; MB15901), glycine (MB01401), BSA (MB04602), NZY colour protein Marker II (MB09002), NZY Tissue gDNA Isolation kit (MB13502), GreenSafe Premium (MB13201), NZYDNA ladder V (MB06101), from NZYTech; ethanol 96% (BP8202-500) and methanol (MeOH; M/4000/17) from Fisher Scientific™; Paraformaldehyde 4% (J61899.AK) and Saponin (J63209) from Alfa Aesar; Nucleic acid sample loading buffer 5x (1610767) from Bio-Rad Laboratories; NucleoSpin® Gel and PCR Clean-up (740609.50) from Macherey-Nagel; Human IL-1β Mini TMB ELISA development Kit (900-T95) from Peprotech.

Antibodies used for immunofluorescence analysis were: anti-human SQSMT1/p62 (SC-28359 AF488, Santa Cruz Biotechnology) at a concentration of 1 µg/mL; anti-human LC3 (0260-100/LC3-2G6, Nanotools) at 5 µg/mL; anti-human NBR1 (MCA3240Z, BioRad) at 2 µg/mL; Goat anti-Mouse IgG (H+L) Cross-Adsorbed Secondary Antibody (A11004, Invitrogen) at 4 µg/mL. Antibodies used for flow cytometry staining were: anti-human

SQSMT1/p62 (SC-28359 AF488, Santa Cruz Biotechnology), at a concentration of 1 µg/mL; Alexa Fluor® 488 Mouse IgG1, κ Isotype Ctrl Antibody (400131, Biolegend), at 2.5 µg/mL. Antibodies used for Western blot were: anti-SQSTM1 Polyclonal Antibody (PA5-20839, Invitrogen), at 10 µg/mL; Monoclonal Anti-β-Actin antibody (A2228, Sigma-Aldrich), at 0.03 µg/mL; Anti-rabbit IgG, HRP-linked Antibody (7074, Cell Signaling Technology), at 0.013 µg/mL; Anti-Mouse IgG, HRP-linked Antibody (715-035-151, Jackson ImmunoResearch), at 0.4 µg/mL.

2.3. Treatment of cells with inhibitors

CAL-1, THP-1 and CAL-1 $p62^{-/-}$ GFP $^{-/-}$ cells were seeded at $1x10^6$ cells/well in 1 ml RPMI 1640 with glutamine with 1% heat-inactivated FBS, 1% Sodium Pyruvate, 1% HEPES and 1% NEAAs, at 37ºC under a 5% CO_2 atmosphere, in one well of a 24-well plate and treated with 10 µM Spautin-1 (autophagy inhibitor; stock solution concentration of 20mM diluted in DMSO) or with 10 µM MG132 (proteasome inhibitor; stock solution concentration of 10 mM diluted in DMSO) for 18 hours.

Regarding the NLRP3-inflammasome inhibition (MCC950), the same seeding conditions were used. In CAL-1 cells, 10 µM of MCC950 (stock solution concentration of 20mM diluted in DMSO) was added to the wells 3 hours before the MG132 treatment. Regarding THP-1 cells, priming with 1 µg/mL of LPS for 6 hours and cell activation with 5 mM of ATP for 18 hours was performed, 10 µM of MCC950 was added 3 hours before cell activation, and in between priming and activation THP-1 were washed and stripped from LPS.

2.4. Generation of p62 knockout cell lines

p62 (SQSTM1) and GFP knockout CAL-1 cells were generated using the CRISPR/Cas9 system as described (86). For generation of p62-deficient CAL-1, cells previously transfected to express Cas9 and GFP under a doxycycline (CAL-1 Cas9 GFP) were used. Guide RNAs (gRNAs) were designed using the GeneArt™ CRISPR Search and Design tool. The gRNAs used were p62 gRNA#1, 5'-AGCCATCGCAGATCACATTG-3'; p62 gRNA #2, 5'-ATGGCCATGTCCTACGTGA-3'; p62 gRNA#3, 5'-GTCATCCTTCACGTAGGACA-3'. gRNA#1 matched a sequence in the third exon, and both gRNA#2 and gRNA#3 matched sequences in the first exon of the target gene. The CAL-1 Cas9 GFP cells were activated

with 2µg/mL of doxycycline, and, 48 hours later, 625,000 cells, in 100µL of medium without FBS, were transduced through electroporation, with 5 µg of each p62 gRNAs and simultaneously a guide RNA for GFP (5'-GAGCTGGACGGCGACGTAAA-3'), using a 4 mm cuvette and the following settings on the electroporator: 350V (875V/cm), 950µF, 25Ω. After electroporation, cells were transferred to a 24-well plate with complete medium (10% FBS and 1% supplements) and 2µg/mL of doxycycline in a total volume of 2.5 mL per well. Two control group were used by transducing the CAL-1 Cas9 GFP cells with only GFP gRNA in one condition and by not performing electroporation in another condition. Individual cell clones, obtained through limiting dilutions, for each p62 gRNA were isolated in 96-well plates and then, after expansion, selected based on lack of GFP and p62 expression, evaluated through flow cytometry. Selected clones were expanded and analysed by Western blot. Furthermore, to determine the mutations of p62 in cloned cells, the genomic sequence around the target region was analysed by Sanger sequencing (LIGHTrun Tube).

2.4.1. Flow Cytometry analyses

Evaluation of GFP expression by flow cytometry was used for an initial selection of clones, since GFP expression of CAL-1 Cas9 GFP cells could be analysed in live cell without any additional fluorescent marker, making the procedure much simpler, considering the large number of clones being manipulated. A lack of expression of GFP suggests a successful knockout of the GFP gene, and thus an increased likelihood for a successful p62 gene knockout. Therefore, clones presenting decreased GFP expression were selected for further analyses and expansion.

Flow cytometry was also used to evaluate expression of p62. Upon collection of 0.5×10^6 cells per condition, they were washed with cold Phosphate-buffered saline (PBS; stock solution composed of 80g NaCl, 14.4g Na_2HPO_4, 2.4g KH_2PO_4 and 3g KCl in distilled water; a dilution of the stock solution at a 1:10 ratio was made to obtain working PBS solution) and fixed with 4% paraformaldehyde for 15 min at room temperature. After washing three times by centrifuging at 300g and at 4ºC for 6 min with excess cold PBS, the cells were permeabilized by resuspension with 1% glycine (1M), 5% FBS and 0.1% Triton™X-100 in PBS (permeabilization solution) and transferred to a U-bottom shape 96-well plate (50µL/well/condition). After plate centrifugation at 400g and at 4ºC for 3 min, the cells were incubated with 50 µL of the appropriate antibody during 1 hour on ice. Then, the cells were washed three times by centrifuging at 400g and at 4ºC for 3 min with excess permeabilization solution plus, an additional final wash by centrifuging at 400g and at 4ºC

for 3 min with excess PBS. Flow cytometry was performed using BD Accuri™ C6 Flow cytometer and the BD AccuriTM C6 Software. A total of 10,000 events were acquired for each sample. Analyses were performed using BD Accuri™ C6 Software (Version 1.0.264.21).

2.4.2. Western blot analysis

For protein analysis, 2×10^6 cells were lysed, for 30 min on ice, using lysis buffer composed by tris buffer with 1% Triton™X-100, half of a tablet of Pierce™ Protease Inhibitor, MG132 at 5 µM, NaF at 50 mM and sodium orthovanadate at 0.2 mM. Lysates were centrifuged for 15 min at maximum speed in a refrigerated (4°C) centrifuge. Proteins were quantified using the BCA (bicinchoninic acid) method (Pierce™ BCA Protein Assay Kit). For such, BSA standards were prepared with concentrations between 2000 µg/mL and 62.5 µg/mL by dilution of the BSA stock solution (2mg/mL), provided by the kit, and then added 20 µL of the different dilution in duplicates in a 96-well plate. Then, in the same 96-well plate, 2 µL of the cell samples, in duplicates, were diluted in water (1:10) and 200 µL of working reagent (50 parts of BCA Reagent A with 1 part of BCA Reagent B, both provided by the kit) was added to all wells. The plate was shaken for 30 seconds and then incubated for 30 min at 37ºC. Absorbance values at 562 nm were measured using Tecan Infinite® 200 Microplate Reader. The plate was shaken for 30 seconds before readings.

To a sample volume corresponding to 20 µg of protein it was added 4 µL of 6x loading buffer and then the volume was adjusted to 24 µL with nuclear-free water. The samples were then heated to 100ºC for 10 min, loaded, and resolved by SDS-PAGE (5 µL of NZY colour protein Marker II (MB09002, Nzytech) was used as a protein marker); The SDS-PAGE mini gel system was composed by a 1.5 mm glass, a comb with the same thickness, running buffer and two types of gels: the resolving gel (10% acrylamide, 30% Tris-HCl 1.5M ph8.8, 2.4% SDS (10% in water), 0.6% APS (10% in water) and 0.06% TEMED in water) where the proteins were separated and the stacking gel (4% acrylamide, 30% Tris-HCl 0.5M ph6.8, 2.4% SDS (10% in water), 0.6% APS (10% in water) and 0.06% TEMED in water) where the samples were loaded. After the gel system was mounted, both gels were polymerized, running buffer was added and the samples and protein marker were loaded, the gel system was run at 90V until the migration front reached the desire level. This was followed by semidry transfer to PVDF membranes at 0.25A (constant) or 16V (constant) for 60 min. Membranes were blocked by incubation with 0.05% Tween and 5% BSA in TBS for 1 hour at room temperature or overnight at 4ºC. After blocking, the membranes were washed with excess 0.05% Tween in TBS and incubated with primary

antibody (SQSTM1, 1:100) overnight at 4ºC. After three thorough washes of 5 min, with excess 0.05% Tween in TBS, membranes were incubated with appropriate anti-rabbit (1:5000) or anti-mouse (1:1000) peroxidase-conjugated secondary antibodies. Even loading was verified and corrected by using β-actin (1:70000, 30 min incubation at room temperature) as a loading control. Lastly, we used the Pierce™ ECL Western Blotting Substrate (32106, Thermo Scientific™) to reveal the membranes. Thus, the membranes were incubated for 5 min with mix detection reagents 1 and 2 at a 1:1 ratio (provided by the kit), at room temperature. Reactive proteins were visualized by chemiluminescent reaction, using the ChemiDoc™ Touch Imaging System.

2.4.3. DNA extraction, purification and sequencing analyses

DNA from CAL-1 $p62^{-/-}$ $GFP^{-/-}$ cell clones was extracted using NZY Tissue gDNA Isolation kit (MB13502, nzytech) based on manufacturer's instructions. We started by resuspending and thoroughly mixing by vortex 1×10^6 cells in 200 µL Buffer NT1 plus 25 µL Proteinase K solution and well mixed 200 µL Buffer NL (all solutions provided in the kit) and incubating the resulting solution at 56ºC for 10-15 min. Then, RNA was removed by adding 10 µL of RNase A solution (40 mg/mL, provided in the kit) to each sample and incubating for 5 min, at room temperature. In the next step, 210 µL of 100% ethanol was added to each sample that were then mixed by vortex and transferred into NZYSpin Column placed in a 2 mL collection tube, centrifuged for 1 min, at 12,000g, and then discarded flow-through. To wash the silica membrane, the samples were centrifuged with 500 µL of buffer NW1 (provided by the kit) at 12,000g at room temperature, the flow-through was discarded and then the same process was repeated but with 600 µL of buffer NW2 (provided by the kit). To dry the silica membrane the empty NZYSpin columns were centrifuged for 2 min at 12.000g, at room temperature. The last step of the DNA extraction was to elute the DNA, so the columns were placed into a clean microcentrifuge tube and 100 µL of TE buffer, preheated to 70ºC, was added directly into the membrane column. The silica membranes were incubated at room temperature for 1 min and then centrifuged at 12,000g for 2 min. The DS-11 Spectrophotometer from DeNovix Inc. was used to quantify the DNA.

A conventional PCR using AmpliTaq Gold 360 Master mix (4398881, ThermoFisher Scientific) was used based on manufacturer's instruction. A mix of 50 µL for each primer pair was prepared with the following components: 25 µL of 2x AmpliTaq Gold master mix, 2 µL of primer forward (at 10µM), 2 µL of primer reverse (at 10µM), 19 µL of Nuclease-free water and 2 µL of template DNA. Then, the tubes were placed in a thermocycler and the following conditions were selected: 1st 95ºC, 10 min; 2nd 40 cycles of 95ºC, 30 sec, followed

by the annealing temperature for 30 sec, followed by 72ºC for 30 sec; 3rd 72ºC, 7 min. For the cells transfected with p62 gRNA#1, the forward primer 5'- GCTCCTTGCTGCTGCTCT-3', the reverse primer 5'-CTGGGGAATGCGAGCTTG-3' and an annealing temperature of 62ºC were used. For the cells transfected with p62 gRNA#2, the forward primer 5'-GGGTAGTCTTGCCTCTCACT-3', the reverse primer 5'-CAAATTGCTGACCCCTTCATT-3' and an annealing temperature of 58ºC were used.

For separation of the PCR products a 1.2% agarose gel with 5 µL of GreenSafe Premium (MB13201, nzytech) was used. 5 µL of the PCR products were mixed with 1 µL of Nucleic acid sample loading buffer 5x (1610767, Bio-Rad Laboratories) and 1.5 µL of NZYDNA ladder V (MB06101, nzytech), as a DNA ladder. Electrophoresis was performed at 95V for 40 min. The detection of the bands was done under an UV trans-illuminator, the Molecular Imager® Gel Doc™ XR+ System with Image Lab™ Software, from BIO RAD.

Purification of PCR products was done through NucleoSpin® Gel and PCR Clean-up (740609.50, Macherey-Nagel), based on manufacturer's instructions. We started by adding 200 µL of buffer NTI (provided in the kit) to 100 µL of each PCR sample, placing a NucleoSpin® Gel and PCR Clean-up Column into a collection tube, loading the sample mixture, centrifuging at 11,000g for 30 sec and discarding the flow-through. Then, the silica membrane was washed with 700 µL of buffer NT3 (provided in the kit), centrifuged at 11,000g for 30 sec and the flow-through was discarded. To dry the silica membrane, the columns were centrifuged at 11,000g for 1 min and the flow-through discarded. The last step was the elution of the DNA, thus, the NucleoSpin® Gel and PCR Clean-up Column were placed into a new 1.5 mL microcentrifuge tube, 20 µL of Buffer NE (provided in the kit) was added followed by an incubation at room temperature for 1 min and a centrifugation at 11,000g for 1 min. The DS-11 Spectrophotometer from DeNovix Inc. was used to quantify the DNA.

Sequencing analyses of the different purified DNA extracts were done by Sanger sequencing (LIGHTrun Tube). For such, the purified DNA extract were diluted (1:3) for a DNA concentration between 20 and 80 ng/µL. The primers were diluted to a final concentration of 5µM. For the cells transfected with p62 gRNA#1, the reverse primer 5'-CTGGGGAATGCGAGCTTG-3' was used, and for the cells transfected with p62 gRNA#2, the reverse primer 5'-CAAATTGCTGACCCCTTCATT-3' was used. A final mixture of 5 µL of the purified DNA extracts with 5 µL of the corresponding primer was prepared, and the samples were sent to sequencing by LIGHTRun.

2.5. Immunofluorescence staining and Confocal Microscopy

After treatment with the inhibitor Spautin-1 or MG132, CAL-1 and CAL-1 p62$^{-/-}$ GFP$^{-/-}$ were seeded at 50,000 cells per 12mm coverslip pre-treated with alcian blue and incubated for 20 min at 37ºC to allow proper attachment. Thereafter, the cells were fixed with 4% paraformaldehyde for 15 min at room temperature. After washing three times in excess PBS, cells were treated with cold MeOH for 5 min at -20ºC, to allow nucleus permeabilization and fixation, followed by three washes with excess PBS. For further permeabilization, PBS containing 1% glycine (1M), 5% FBS and 0,1% Triton™X-100 was used, followed by a wash with staining buffer composed by 1% glycine (1M) and 5% FBS in PBS. Samples were then incubated for 1h at room temperature, first with the primary antibody, then with the fluorescent secondary antibody and finally with the conjugated primary antibody. When necessary, DAPI (300 nM) staining was used for nuclear counterstaining. Between each antibody incubation, the cells were washed three times with excess staining buffer. Image acquisition was performed using the confocal microscope Zeiss LSM 510 META, in the LiM facility of iBiMED, a node of PPBI (Portuguese Platform of BioImaging): POCI-01-0145-FEDER-022122.

2.5.1. Image processing

After acquisition, ImageJ software – Fiji processing package - and related plugins were used for image processing and co-localization. The images were obtained through focus stacking, so, in order to analyse all the aggregates, the plugin Stk → Z Project was used. The count of aggregates per cell was done manually. The area of the aggregates was determined by adjusting the aggregates' threshold and then using the plugin Analyse → analyse particles after selecting "Area" in Analyse → Set Measurements. To analyse co-localization, individual cells were cropped and the plugin JACoP was used to quantify the Pearson's Coefficient.

2.6. ELISA

Culture supernatants were collected after treatment with inhibitors for different timepoints and subjected to ELISA to detect secreted IL-1β protein using a Human IL-1β Mini TMB ELISA development Kit (900-T95, Peprotech). The capture antibody (100 µg/mL), detection antibody (100 µg/mL) and Human IL-1β Standard (1 µg/mL) were reconstituted in

sterile water. Streptavidin-HRP Conjugate (100 µg/mL) was reconstituted in PBS. The first step was the dilution of the capture antibody in PBS to a concentration of 0.25 µg/mL and the overnight incubation of the desired ELISA plate wells with 100 µL of the diluted antibody. Then, the wells were blocked for 1 hr with 300 µL of block buffer (provided in the solutions kit). After blockage, the standard was diluted with diluent (provided in the solutions kit) in a series of solutions from 750 pg/mL to zero, in triplicate wells of 100 µL. Then, 100 µL of sample was added to each corresponding well and the plate was incubated for at least 2 hours. In the next step, the detection antibody was diluted with diluent to a concentration of 0.25 µg/mL and the wells were incubated with 100 µL of the diluted antibody for at least 2 hours. Thereafter, the Streptavidin-HRP was diluted with diluent to a concentration of 0.1 µg/mL and the wells were incubated with 100 µL of the diluted conjugate for 30 min. The two last steps were to add 100 µL of TMB liquid substrate (provided in the solutions kit) to each well, incubate for 20 min and then stop the reaction with 100 µL of 1M HCL Stop Solution (provided in the solutions kit). All incubations were done at room temperature with low plate agitation and, in between every incubation, the ELISA plate was washed 4 times with wash buffer (provided in the solutions kit), except in the two last steps where it was not used agitation and wells were not washed in between the steps. Absorbance values were measured using Tecan Infinite® 200 Microplate Reader.

2.7. ProteoStat staining assay

A ProteoStat® aggresome detection kit (Enzo life sciences Inc.) was used to analyse the presence of aggregates. Cells were washed with PBS and fixed with 4% paraformaldehyde for 15 min at room temperature, with the centrifugations done at 300g and 4ºC for 6 min. After being washed three times with excess cold PBS, the cells were permeabilized with 200 µL of 0.1% saponin, 0.5% BSA, 0.01% sodium azide in PBS and centrifuged. The cells were then resuspended with ProteoStat dye diluted 1:4000 in the permeabilization solution for 30 min at room temperature protected from light. Flow cytometry was preformed using BD Accuri™ C6 Flow cytometer and the BD Accuri™ C6 Software. A total of 10,000 events were acquired for each sample. Analyses were performed using BD Accuri™ C6 Software (Version 1.0.264.21).

2.8. Viability test

Cell viability was evaluated through a dye exclusion test. CAL-1 and THP-1 cells were subjected to MG132 inhibition, as described before, using various concentration of MG132 (5, 7.5 and 10 µM) and timepoints (4, 6, 8, 10, and 18 hours). An MG132 pre-treatment was also performed, where cells were inhibited with 10 µM MG132 for 8 hours and then were stripped from the drug and incubated in fresh cell medium for another 18 hours, with cell viability being evaluated in both timepoints. After treatment, the cells were stained with Trypan Blue Solution (Sigma-Aldrich) and an hemocytometer was used to count the viable and dead cells.

2.9. Evaluation of plasma-membrane integrity: LDH Cytotoxicity Assay

To assess the percentage of disruption of the cell plasma-membrane caused by MG132 treatment on CAL-1 and THP-1 cells, a reliable colorimetric method was used: the cyQUANT™ LDH Cytotoxicity Assay Kit, from Invitrogen (C20300), that uses Lactate dehydrogenase (LDH) concentration in media as an indicator of cellular cytotoxicity. The procedure was done according to manufacturer's instructions. Firstly, the optimum cell number for the LDH cytotoxicity test was determined. A serial dilution of cells (0-10,000 cells/ 100 µL of media) in two sets of triplicate wells in a 96-well tissue culture plate were prepared. One set was used to determine the Maximum LDH Release while the second set was used to determine the Spontaneous LDH release. After an overnight incubation at 37ºC in a 5% CO_2 atmosphere, 10 µL of sterile water was added to the Spontaneous LDH Release set of dilution series and 10 µL of Lysis Buffer was added to the Maximum LDH Release set of dilution series and the plate was incubated in the same conditions for 45 min. Thereafter, 50 µL of each sample was transferred to a 96-well flat bottom plate, 50 µL of Reaction Mixture (provided in the kit) was added to each sample well, and the plate was incubated at room temperature for 30 min, protected from light. The reaction was stopped by adding 50 µL of Stop Solution to each sample well. Absorbance values were measured using Tecan Infinite® 200 Microplate Reader.

Afterwards, the chemical compound-mediated cytotoxicity was performed; Three sets (Spontaneous LDH Activity, Maximum LDH Activity and Chemical-treated LDH activity) of CAL-1 cells, in triplicate, were plated at 8.000 cells/well in 100µL of RPMI 1640 with glutamine with 1% heat-inactivated FBS, 1% Sodium Pyruvate, 1% HEPES and 1% NEAAs,

on a 96-well tissue culture plate; The chemical-treated cells were treated with either 10 µL of 10 µM MG132 for 18 hours or with 10 µL of 10 µM of MCC950 for 3 hours before adding 10 µL of 10 µM of MG132 for an additional 18 hours, at 37ºC in a 5% CO_2 atmosphere. To the "Spontaneous LDH Activity" set of cells was added 10 µL of sterile water at the same time that MG132 was added to the chemical-treated cells. Regarding the "Maximum LDH Activity" set of cells, 45 min before the end of incubation of the chemical-treated cells, 10 µL of Lysis buffer were added. Thereafter, 50 µL of each sample were transferred to a 96-well flat bottom plate, 50 µL of Reaction Mixture were added to each sample well, and the plate was incubated at room temperature for 30 min, protected from light. The reaction was stopped by addition of 50 µL of Stop Solution to each sample well. Absorbance values were measured using Tecan Infinite® 200 Microplate Reader.

2.10. Statistics

Statistical analysis was performed using GraphPad Prism 8.0.2 software. Values are presented as means (±SEM) from at least three independent experiments, unless mention otherwise. Considering that the sample size obtained is small, and that data is not normally distributed, a nonparametric test was used for statistical analyses. Therefore, data were analysed by Kruskal-Wallis test to determine statistically significant differences between treatment groups: *, $p<0.05$: **, $p<0.01$; ****, $p<0.0001$.

3. Results

3.1. Inhibition of autophagy or the proteasome promotes accumulation of protein aggregates with different characteristics

Protein aggregation can be induced by a wide variety of cellular stresses. The impact of either inhibition of autophagy or inhibition of the proteasome on accumulation of protein aggregates in a cell model of human pDC was thus analysed. With this goal in mind, CAL-1 cells were treated with Spautin-1 (an autophagy inhibitor) or MG132 (a proteasome inhibitor) and two different approaches were adopted to detect protein aggregates: the Proteostat™ Protein Aggregation Assay was used to detect protein aggregation by flow cytometry; and Laser Scanning Confocal Microscopy was used for direct visualization of protein aggregates, attainable by using appropriate markers. Regarding the Proteostat™ Protein Aggregation Assay, proteasome inhibition led to a more pronounced increase in the proteostat fluorescence that autophagy inhibition (Figure 2). Thus, while both autophagy and proteasome inhibition in CAL-1 induced protein aggregation, proteasome inhibition resulted in a superior response.

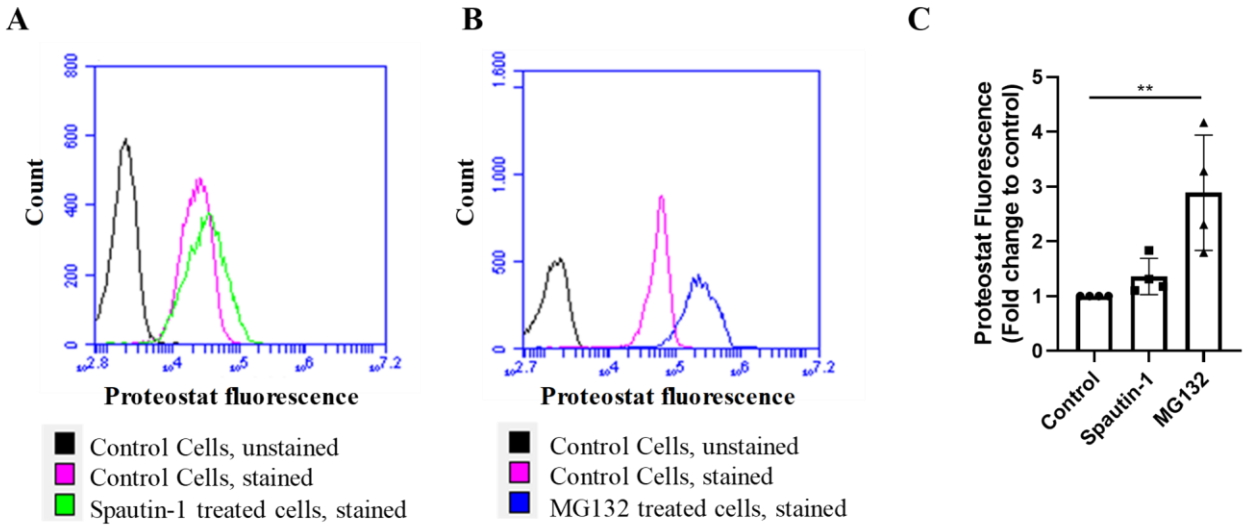

Figure 2 Evaluation of protein aggregation by flow cytometry upon autophagy or proteasome inhibition. (A) and (B) Flow cytometry histograms showing Proteostat fluorescence intensity in CAL-1 cells treated with Spautin-1 for 19 hours **(A)** or with MG132 for 18 hours **(B)**. Data is representative of four experiment. **(C)** Proteostat fluorescence intensity from Spautin-1 or MG132 treated CAL-1 cells relative to control cells. Graph shows average ± SEM, with n=4. Kruskal-Wallis test was performed to determine statistically significant: **, $p < 0.01$ compared to the control cells.

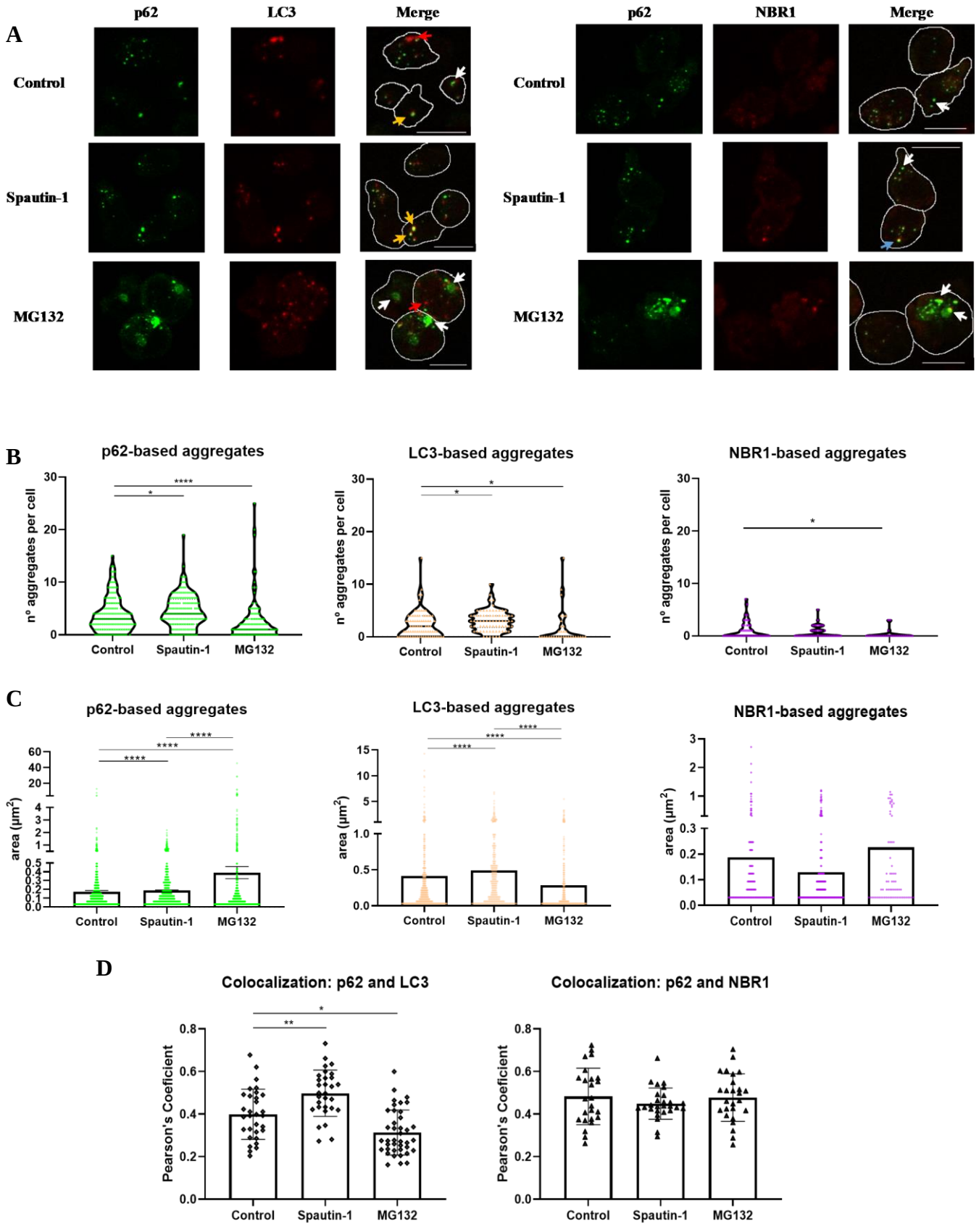

Figure 3 Analysis of protein aggregates by confocal microscopy upon autophagy or proteasome inhibition. Subtitle in the next page.

Figure 3 Analysis of protein aggregates by confocal microscopy upon autophagy or proteasome inhibition. (A) p62, LC3 (right panel) and NBR1 (left panel) were visualized upon CAL-1 cells treatment with either 10µM of Spautin-1 for 19 hours or 10µM of MG132 for 4 hours. The white arrows show p62-aggregates, the red arrows show LC3-aggregates, the yellow arrows show p62 and LC3-aggregates and the blue arrow show p62 and NBR1-aggregates. The scale corresponds to 10µm. **(B), (C) and (D)** protein aggregates composition and morphology. Analyses of confocal microscopy images were done with ImageJ software. **(B)** number of p62-, LC3- and NBR1-based aggregates per cell. **(C)** area of each individual p62-, LC3- and NBR1-based aggregate in μm^2. **(D)** colocalization of p62 with LC3 or p62 with NBR1, calculated using Pearson's coefficient **(B), (C) and (D)** Values are presented as a violin plot (**B**), mean (**C**) and mean ± SEM (**D**). number of cells per condition between 111 and 201. Kruskal-Wallis test was performed to determine statistical differences: *, p<0.05, **, p<0.01 and ****, p<0.0001, compared to the control cells.

Thereafter, we performed confocal microscopy immunofluorescence analyses of p62, a marker for DALIS (29), LC3, an autophagosome marker (87), and NBR1, a marker for protein aggregates in general (88), with the objective of studying the composition and morphology of the protein aggregates induced by autophagy or proteasome inhibition. Similarly to what was done before, CAL-1 cells were analysed after Spautin-1 or MG132 treatment (Figure 3A). Cells treated with an autophagy inhibitor had a higher number of p62- and LC3-based aggregates per cell than cells treated with a proteasome inhibitor, while the number of NBR1-based aggregates did not change significantly (Figure 3B). This was accompanied by a slight but significant increase in the area of the LC3-based aggregates (Figure 3C), and a more evident colocalization of p62 and LC3 in Spautin-1 treated cell (Figure 3D). On the other hand, proteasome inhibition with MG132 led to a decrease in the number of p62-, LC3- and NBR1-based aggregates (Figure 3B). But interestingly, while the area of LC3-based aggregates decreased, the area of p62-based aggregates showed a clear increase (Figure 3A and 3C), with p62 clearly accumulating in more prominent and larger aggregates. Additionally, the colocalization of p62 and LC3 decreased in MG132 treated cells (Figure 3D). Collectively, these results indicate that autophagy inhibition with Spautin-1 in pDCs induce formation of autophagosomes, while proteasome inhibition in pDCs results in accumulation of p62 leading to formation of fewer but larger and prominent p62-based aggregates.

3.2. Proteasome inhibition induces an inflammatory response by CAL-1 cells

In order to correlate protein aggregation with the inflammatory response, and because autophagy and proteasome inhibition induced protein accumulation in different types of aggregates (Figure 3), secretion of the proinflammatory cytokine IL-1β was quantified after

treating CAL-1 cells with Spautin-1 or MG132. Importantly, IL-1β secretion was significantly increased in MG132 treated CAL-1 cells (Figure 4A). Inhibition of autophagy promoted a smaller, and not significant increase in secretion of IL-1β (Figure 4A). This effect was not observed with the monocytic cell line THP-1 (Figure 4B). Therefore, our results suggest that proteasome inhibition induces IL-1β secretion in pDCs in a cell specific manner.

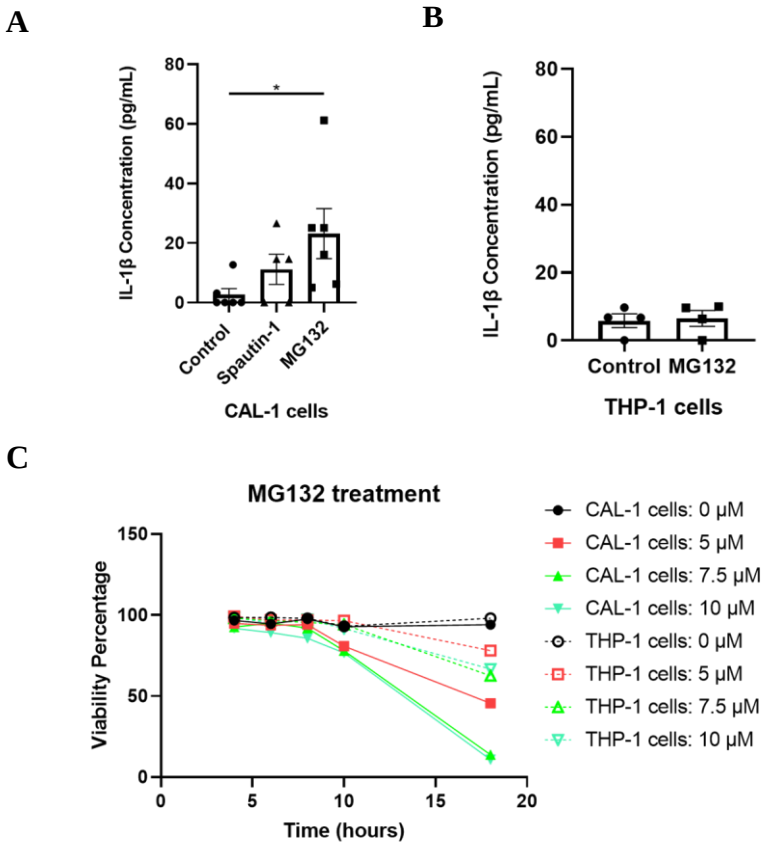

Figure 4 Evaluation of the effects of autophagy or proteasome inhibition in IL-1β secretion and cell viability. (A) and (B) supernatants were collected from CAL-1 **(A)** or from THP-1 **(B)** cells after 18 hours of Spautin (10 μM) or MG132 (10 μM) treatment and used for measurement of secreted IL-1β by ELISA. **(C)** cell viability was evaluated through a dye exclusion test, using Trypan Blue Solution. **A.** CAL-1 and THP-1 were treated with either 0, 5, 7.5 or 10 μM of MG132. Cell viability was evaluated after 4, 6, 8, 10 and 18 hours of incubation. **(A), (B) and (C)** Values are presented as mean ± SEM with n=6 **(A),** n=4 **(B)** and n=1 **(C).** Kruskal-Wallis test was performed to determine statistically significant: *, $p<0.05$ compared to the control cells.

Pyroptosis is a form of programmed cell death associated with the inflammatory response. Pyroptosis requires the function of the enzyme caspase-1 and subsequently is associated with an increased maturation and secretion of IL-1β and IL-18 (89). To investigate the impact of proteasome inhibition on CAL-1 viability, cells were incubated with different concentrations of MG132 for various time points before quantifying cell death with

a trypan blue exclusion test. Interestingly, proteasome inhibition induced drastic CAL-1 cell death, regardless of the MG132 concentration, after 18 hours of incubation (Figure 4C). Again, this effect was cell specific, as cell viability of THP-1 cells remained considerably higher after 18 hours of MG132 treatment (Figure 4C). Parallel work in our lab also showed, with the LIVE/DEAD™ Fixable Far-Red Dead Cell Stain assay, that CAL-1 cell viability declined over time while THP-1 cell viability stayed constant upon proteasome inhibition (Supplementary Figure 1).

In order to understand if the effects of proteasome inhibition observed in pDCs are reversible, after treating cells with MG132 for a period of 8 hours, cells were washed, and allowed to recover for 18 more hours. At the end of the initial 8 hours of proteasome inhibition, CAL-1 cells displayed a high viability percentage (Figure 5C) and were secreting a low quantity of IL-1β (Figure 5A). Interestingly, at the end of the 18 hours of rest, even though the cells had been stripped from MG132, CAL-1 cells displayed a drastically low viability percentage (Figure 5C) and IL-1β continued being secreted (Figure 5A). Once again, the same effect was not observed with the THP-1 cells (Figure 5B and 5C). Together, these results lead us to believe that proteasome inhibition in pDCs, besides leading to IL-1β secretion, also induce cell death in a cell specific and irreversible manner.

3.3. NLRP3 inflammasome is not activated by proteasome inhibition in pDCs

Proteasome inhibition induced both cell death and IL-1β secretion in pDCs, suggesting that proteasome inhibition induced inflammasome activation and, ultimately, pyroptosis. With this hypothesis in mind, we then tested the involvement of the NLRP3-inflamassome in the secretion of IL-1β mediated by proteasome inhibition in pDCs. Thus, we used the drug MCC950, an NLRP3-inflammasome inhibitor. As expected, IL-1β secretion significantly decreased in primed and activated THP-1 cells treated with MCC950 (Figure 6A), indicating a successful NLRP3-inflammasome inhibition. Unfortunately, CAL-1 cells secreted IL-1β in basal conditions, contrary to our previous data, and thus inhibition of the proteasome in CAL-1 cells did not induce an increased IL-1β secretion, compared to control cells (Figure 6B), which jeopardized any conclusions regarding the effect of NLRP3 inhibition. Nevertheless, analysing the fold change on IL-1β concentration upon MCC950 treatment relative to vehicle (DMSO) treatment suggests that the NLRP3-inflammasome is not involved in the IL-1β secretion that was observed (Figure 6C).

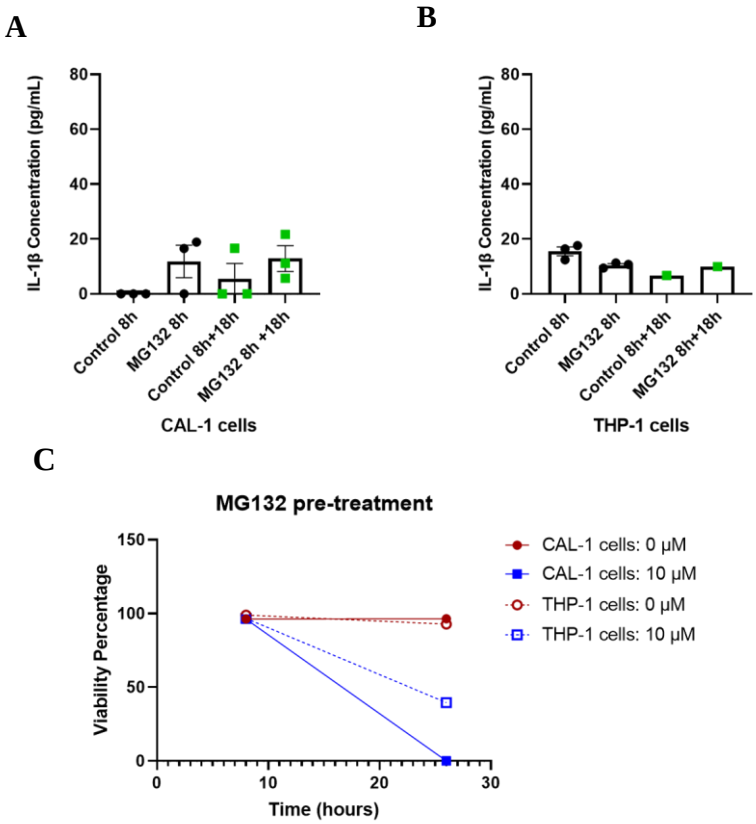

Figure 5 Evaluation of IL-1β Secretion and cell viability upon MG132 pre-treatment. (A) and (B) CAL-1 **(A)** and THP-1 **(B)** cells were incubated with 10 µM of MG132 for 8 hours and supernatants were collected. The cells were then washed and incubated for 18 more hours with fresh medium for a new supernatants collection. Collected supernatants were used for measurement of secreted IL-1β by ELISA. **(C)** cell viability was evaluated through a dye exclusion test, using Trypan Blue Solution. CAL-1 and THP-1 cell were incubated with 0 or 10 µM of MG132 for 8 hours and cell viability was evaluated. The cells were then washed and incubated for 18 more hours with fresh medium for a new cell viability evaluation. **(A), (B), and (C)** Values are presented as mean ± SEM with n=3 **(A) and (B)** and n=1 **(C).** Kruskal-Wallis test was performed to determine statistically significant: *, $p<0.05$ compared to the control cells.

Regarding the effect of proteasome inhibition in pDCs death, NLRP3-inflammasome inhibition did not alter the significant reduction observed on CAL-1 cell viability upon treatment with MG132 (Figure 7A). One of the primary characteristics that distinguish pyroptosis from apoptosis is the disruption of the plasma-membrane that occurs upon inflammasome activation. Leakage of intracellular molecules, such as LDH, through the impaired plasma-membrane can be used to detect damage of the plasma-membrane, thus we used the cyQUANT™ LDH Cytotoxicity Assay Kit to evaluate plasma-membrane integrity. After determining the optimum number of cells to use in this assay (Supplementary Figure 2), CAL-1 cells were treated with MG132 or both MG132 and the NLRP3-inflammasome inhibitor. Proteasome inhibition did not induce an increase in cytotoxicity (Figure 7B), which indicates that the integrity of the plasma-membrane was not disrupted.

Together, these results suggest that proteasome inhibition in CAL-1 cells induces cell death through a mechanism other than pyroptosis.

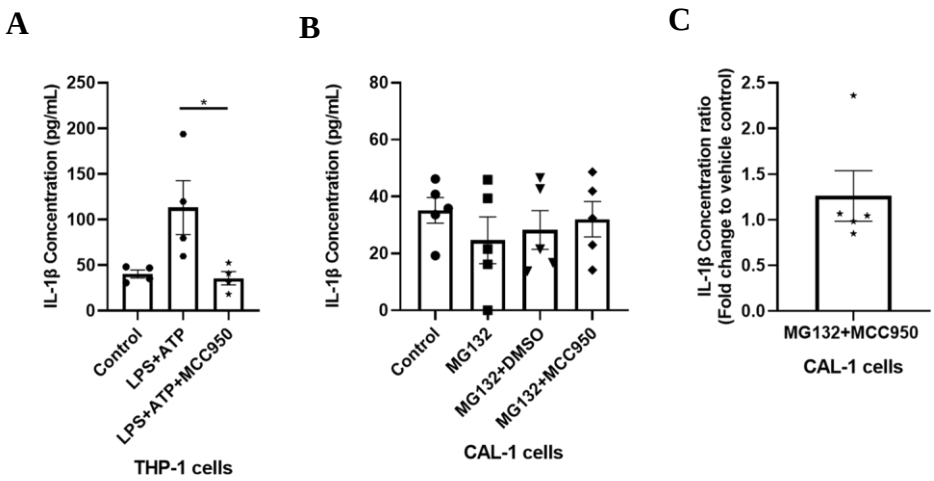

Figure 6 NLRP3 inflammasome does not mediate IL-1β secretion after proteasome inhibition. (A) THP-1 cells were primed with 1 µg/mL of LPS for 6 hours and activated with 5 mM of ATP for 18 hours. Three hours before THP-1 activation, 10 µM of MCC950 was added for inflammasome inhibition. **(B)** CAL-1 cells were incubated with 10 µM of MCC950 for 3 hours and then 10 µM of MG132 was added for an incubation of 18 more hours. DMSO was used as the vehicle control. **(A) and (B)** supernatants were collected after MG132 or MG132 and MCC950 treatment and used for measurement of secreted IL-1β by ELISA. Values are presented as mean ± SEM. *, p<0.05 compared to the control cells. **(C)** fold change of IL-1β concentration upon MG132+MCC950 treatment relative to vehicle (DMSO) treatment. **(A), (B) and (C)** Graph shows average ± SEM with n=4 **(A)** and n=5 **(B) and (C)**. Kruskal-Wallis test was performed to determine statistically significant: *, p<0.05 compared to the control cells.

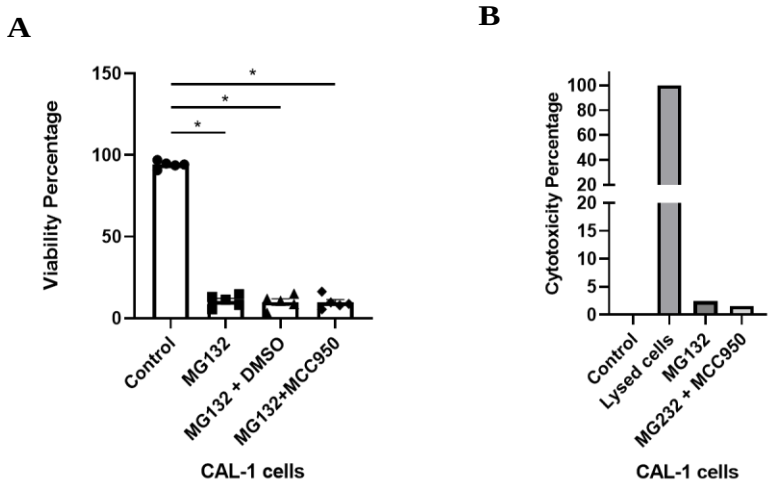

Figure 7 Proteasome inhibition in pDCs promotes cellular death but not pyroptosis. (A) and (B) CAL-1 cells were incubated with 10 µM of MCC950 for 3 hours and then 10 µM of MG132 was added for an incubation of 18 more hours; DMSO was used as the vehicle control **(A)** cell viability was evaluated through a dye exclusion test, using Trypan Blue Solution. **(B)** supernatants were collected after treatment and used for measurement of LDH concentration in media by cyQUANT™ LDH Cytotoxicity Assay Kit. (**A) and (B)** Values are presented as mean ± SEM, with n=5 **(A)** and n=1 **(C).** Kruskal-Wallis test was performed to determine statistically significant: *, p<0.05 compared to the control cells.

3.4. p62 is not essential for pDCs response to proteasome inhibition

Earlier we observed that proteasome inhibition in pDCs induced accumulation of p62-based aggregates. To understand the role of these aggregates in pDCs inflammatory response, we created p62 knockout (KO) CAL-1 cell lines. The generated cell lines (p1.4, p2.7 and p2.8) showed a decreased staining of p62 by flow cytometry (Figure 8A) and absence of p62 labelling by Western blotting (Figure 8B). Genomic sequencing confirmed that the three selected clones were successfully genetically edited (Figure 9).

A

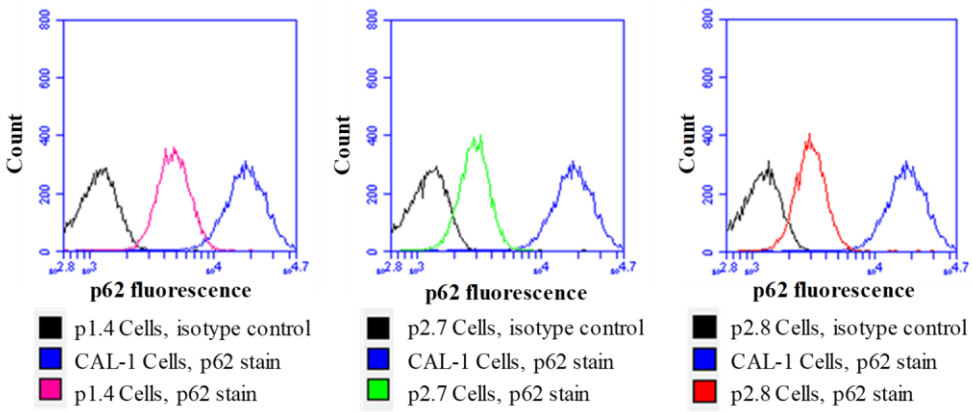

B

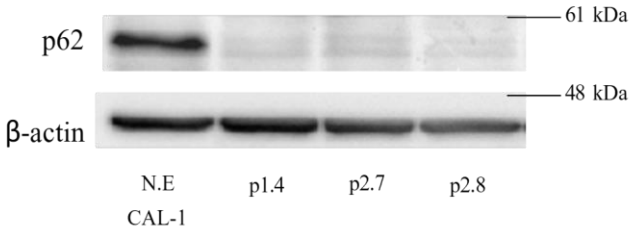

Figure 8 p62 knockout CAL-1 cell lines. p62 knockout (KO) cell clones were independently generated by CRISPR/Cas9 system. **(A)** Flow cytometry histograms showing p62 fluorescence intensity in p62 KO CAL-1 cells **(B)** Protein extracts from individual p62 KO clones were analysed by Western blot for p62 and β-actin.

After successfully obtaining three different p62 KO CAL-1 cell lines (p1.4, p2.7 and p2.8), we inhibited either the proteasome or autophagy, as on previous experiments, and studied IL-1β secretion and cell viability. All three p62 KO clones showed an increased IL-1β secretion in all three conditions (control, autophagy inhibition and proteasome inhibition) (Figure 10A). However, CAL-1 cells were secreting IL-1β in all three conditions as well (Figure 10A), contrarily to what was previously observed (Figure 4A), jeopardizing any conclusion on the role of p62 on IL-1β secretion results. Concerning the evaluation of cell

viability, proteasome inhibition induced drastic cellular death on all three p62 KO clones, as well as on CAL-1 cells (Figure 10B). These results suggest that the p62-based aggregates formed upon proteasome inhibition were not involved in the cell death observed in pDCs upon proteasome inhibition.

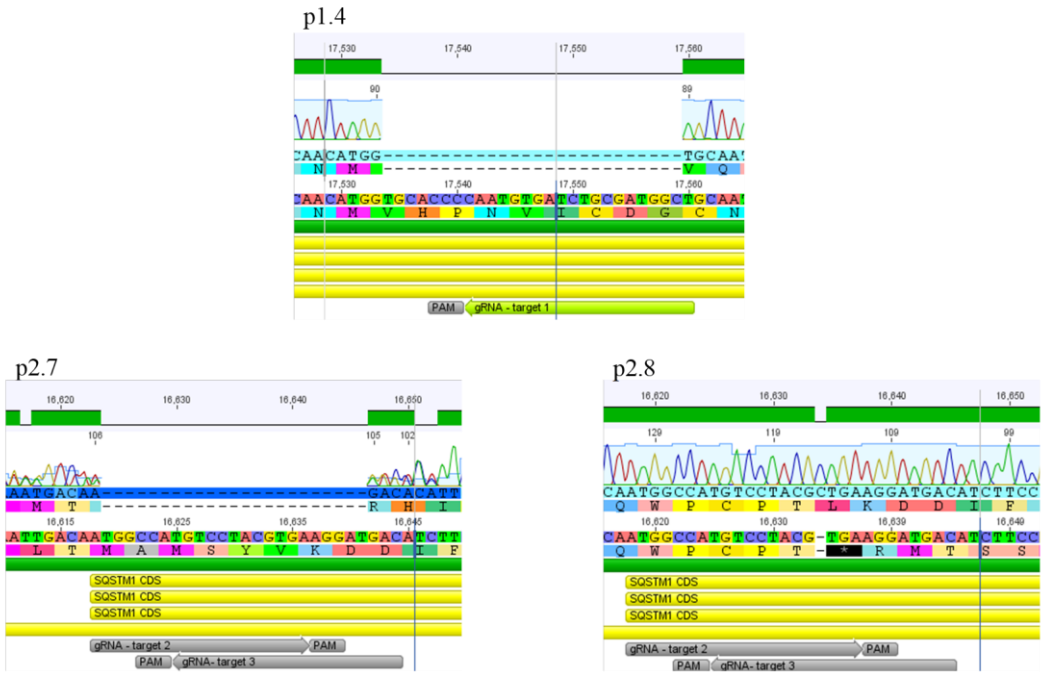

Figure 9 Sequencing of p62 knockout CAL-1 cell lines. Genome sequence of the gRNAs' targets for the selected p62 knockout clones, analysed by Sanger sequencing. Sequencing analyses demonstrates the following mutations on the coding sequence of the targeted exons on each clone: a deletion of 26 nucleic bases on clone p1.4; a deletion of 23 nucleic bases on clone p2.7; an insertion of 1 nucleic base on clone 2.8. The alterations observed are, in all three clones, nonsense mutations that induce a truncated, incomplete, and nonfuctional protein product.

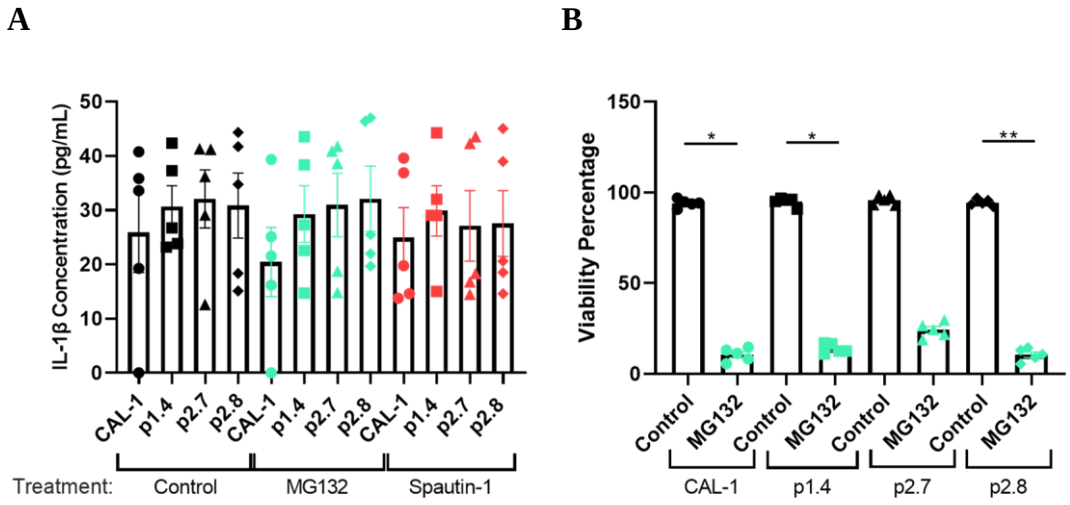

Figure 10 Role of p62 in CAL-1 cells response to proteasome inhibition. (A) and (B) CAL-1 and p62 knockout CAL-1 cells clones (p1.4, p2.7 and p2.8) were treated with 10 µM of MG132 for 18 hours **(A)** supernatants were collected after treatment and used for measurement of secreted IL-1β by ELISA. **(B)** Cell viability was evaluated through a dye exclusion test, using Trypan Blue Solution. **(A) and (B)** Values are presented as mean ± SEM with n=5. Kruskal-Wallis test was performed to determine statistically significant: *, $p<0.05$ and **, $p<0.01$ compared to the control cells.

4. Discussion

The primary aim of this study was to understand if protein accumulation plays a role in pDCs inflammatory response. It was found that proteasome inhibition in pDCs induced both accumulation of p62-based aggregates and inflammation, in the form of IL-1β secretion and cell death, in a cell specific and irreversible way. However, the effect of proteasome inhibition on cell viability occurred independently of the presence of p62. Furthermore, IL-1β secretion induced by proteasome inhibition was independent of the NLRP3-inflammasome and the cell death observed was not pyroptosis.

Inhibition of either autophagy or the proteasome in pDCs led to accumulation of protein aggregates with a different morphology. The presence of LC3 in the protein aggregates induced by autophagy inhibition suggests that the protein aggregates observed are autophagosomes, since LC3 is a well described maker for autophagosomes (87).

It has been shown that p62 accumulates alongside DRiPs in (D)ALIS, being that p62 is an essential protein for (D)ALIS formation (29). Furthermore, DALIS are transient in nature and can be rapidly detected upon stimuli (18,21). Here, p62-based aggregatescould be detected as soon as 4 hours upon proteasome inhibition (Figure 3). Various studies show that the proteasome is not implicated in the assembly of (D)ALIS but, on the contrary, its activity is linked to the clearance of these aggregates (18,33). Indeed, proteasome inhibition seems to enhance accumulation of ubiquitinated proteins and DALIS formation in DCs (18,23). Therefore, the p62-based aggregates observed upon proteasome inhibition in pDCs have the potential to be considered DALIS, but further studies where the transient profile of the aggregates is tested and more DALIS markers are used, such as for polyubiquitin, need to be done to confirm this hypothesis.

Interestingly, our data indicate that proteasome inhibition induces an inflammatory response by pDCs in the form of IL-1β secretion (Figure 4A). Previous studies show that proteasome inhibition in cDCs has a highly anti-inflammatory effect since, for instance, it inhibits NF-κB activation, it reduces the secretion of immunostimulatory cytokines, such as IL-12 and TNF-α upon LPS stimulation, and it prevents the upregulation of costimulatory molecules, thus strongly disturbing cDC immunogenicity (75,77,78). Concerning pDCs, it has been shown that proteasome inhibition impairs the immunostimulatory capacity of this type of cell, by disruption of ER homeostasis, that also impairs cell viability (80). This is in agreement with our data, where proteasome inhibition led to a significant and severe

decrease in pDCs cell viability (Figure 4C). In contrast, our results regarding IL-1β secretion mediated by proteasome inhibition in pDCs are not in agreement with the available literature. Both the increased IL-1β secretion and the decreased cell viability effect was not observed upon proteasome inhibition in the monocytic cell line (THP-1) (Figure 4B and Figure 4C) indicating that pDCs respond to proteasome inhibition in a specific manner. To further elucidate the effects of proteasome inhibition in pDCs, we studied the reversibility of the MG132 treatment in pDCs. MG132 is described as a potent, reversible and cell permeable proteasome inhibitor (90). However, our attempt to reverse the MG132 treatment showed that the effects mediated by proteasome inhibition in pDCs are irreversible. In fact, even though CAL-1 cells were stripped from MG132 before significant IL-1β secretion or cell viability being affected (Figure 5A and C), the pre-treated pDCs still showed the effect of proteasome inhibition after the attempted recovery, with increased IL-1β secretion (Figure 5A) and drastic cell death (Figure 5C). These results indicate that proteasome inhibition in pDCs initiates an effect chain that cannot be stopped by recuperation of proteasome activity, and therefore, pDCs respond to proteasome inhibition in a cell specific and irreversible type manner.

IL-1β secretion is reliant on inflammasome activation, as caspase 1 has to be active in order to occur maturation of the IL-1β proform and subsequent release of mature IL-1β (54). Interestingly, we showed that the activity of the NLRP3-inflammasome is not essential for the IL-1β secretion observed in pDCs upon proteasome inhibition (Figure 6C), thus suggesting the involvement of an alternative inflammasome, such as the AIM2-inflammasome, an inflammasome that is usually triggered by nucleic acids (91), or maybe other non-conventional forms of IL-1β secretion.

While trying to understand the role of NLRP3-inflammasome in IL-1β secretion mediated by proteasome inhibition, we were faced with a problem regarding IL-1β secretion. Unexpectedly, CAL-1 cells secreted IL-1β under basal conditions (Figure 6B), indicating that control CAL-1 cells were being activated. This reaction was specific to CAL-1 cells, since THP-1 cells were not being activated under control conditions (Figure 6A). Moreover, upon priming and activation, THP-1 cells reacted as expected to NLRP3-inflammasome inhibition by significantly decreasing the levels of secreted IL-1β (Figure 6A). By gathering all our results concerting IL-1β secretion by CAL-1 cells (Supplementary Table 1) we can see an evident change in behaviour after July 30th. It was from this date on that CAL-1 cells began to secrete IL-1β in basal condition. It is possible that this difference is due to the fact that the FBS batch used in our cell medium was changed (from Lot: BCVQ9326V, Sigma

to Lot: BCCB5187, Sigma). The FBS levels of hormones, lipids, and proteins can vary widely from lot to lot. This complex variety has important implications for cell culture, as each cell type has its unique requirements, even being able to impact cellular function. Therefore, we believe that the newly used FBS induced CAL-1 activation and, consequently, led to IL-1β secretion. To confirm our suspects, we will need to run an FBS test, where we will use different brands and batches of FBS, and we will test how the different types of FBS affect the basal level of IL-1β secretion in CAL-1 cells. Another possible explanation would be medium contamination with bacteria capable of activating the CAL-1 cells, but that seems unlikely since there were no visible signs of contamination and, also, different vials of CAL-1 cells were used in the various assays. Considering this, new assays must be performed to confirm the results obtained in regard to IL-1β secretion in CAL-1 cells after both NLRP3-inflammasome and proteasome inhibition.

The canonical pathway for IL-1β production requires activation of caspase-1 containing inflammasomes for pro-IL-1β processing followed by pyroptosis, a highly pro-inflammatory form of programmed cell death (92). Pyroptosis depends on caspase-1 activation and is characterized by plasma-membrane rupture and release of proinflammatory intracellular contents, such as IL-1β (89). NLRP3-inflammasome inhibition did not rescue pDCs from proteasome inhibition-mediated cell death (Figure 7A), suggesting that the NLRP3-inflammasome is not essential for this response. Furthermore, the cell death detected in pDCs upon proteasome inhibition is not associated with cell membrane disruption (Figure 7B), indicating that the cell death observed is not pyroptosis. Considering that caspase-1 activation induces pyroptosis and that proteasome inhibition in pDCs leads to IL-1β secretion but not pyroptosis, our results suggest that the IL-1β secretion, observed upon proteasome inhibition in pDCs, is independent of activation of caspase-1 containing inflammasomes. Thus, proteasome inhibition induces a non-conventional form of IL-1β secretion in pDCs. Recently, it has been shown that the apoptotic caspase-8 is also capable of proteolytically processing pro-IL-1β into its active form, either directly or via the NLRP3 inflammasome, in bone marrow-derived DCs (92,93). Thus, we hypothesize that proteasome inhibition in pDCs mediates caspase-8 activation that, subsequently, directly maturates IL-1β and ultimately leads to apoptosis. To confirm our hypothesis more studies need to be conducted. Future work will aim to detect apoptosis, for example with the annexin V / Propidium Iodide apoptotic assay that can be used to detect both apoptosis and necrosis by flow cytometry. Also, a caspase-8 inhibitor, such as Z-IETD-FMK, will be used to study the role of caspase-8 in IL-1β secretion mediated by proteasome inhibition.

p62 (also known as SQSTM1) is a multifunctional stress-inducible scaffold protein involved in various biological responses, including tumorigenesis, apoptosis, inflammation and autophagy (94). In particular, p62 links the autophagy pathway and the ubiquitin-proteasome system, by acting like a bridge that activates autophagy when proteasome inhibition occurs (95). In the present study, we observed that proteasome inhibition in pDCs leads to accumulation of p62-based aggregates (Figure 3) as well as IL-1β secretion (Figure 4A) and cell death (Figure 4C). Taking these results into account, we created a CAL-1 cell line knocked out for p62 (Figure 8 and 9). The null expression of p62 (Figure 8B), as a consequence of the mutated p62 gene (Figure 9), allows us to study its role in the pDCs response to proteasome inhibition. All three selected CAL-1 p62 KO clones (p1.4, p2.7 and p2.8) presented proteasome inhibition-mediated cell death, as CAL-1 cells (Figure 10B), suggesting that p62 does not play a role in the observed pDCs death mediated by proteasome inhibition. Due to the lack of a negative control (since the control CAL-1 cell started secreting IL-1β in basal conditions, as previously mentioned), our results on p62 KO clones IL-1β secretion were inconclusive. Thus, new assays must be performed for a better understanding of the role of p62 on pDC mediated inflammatory response.

4.1. Limitations

The findings of this study must be seen in light of some limitations. The primary limitation to the generalization of these results is the fact that there were obtained with a cell line. Immortal cell lines offer several advantages, such as being cost-effective, easy to use and a consistent material that avoids ethical concerns associated with the use of animal and human tissue. However, the use of cell lines in replace of primary cells must be done carefully. Cell lines are genetically manipulated, and serial passage of cell lines can further cause genotypic variation, which could lead to alterations on their phenotype, native functions and their responsiveness to stimuli. Therefore, cell lines may not adequately represent primary cells and may provide different results that can induce false conclusions. Other problems associated with cell lines are contamination with other cell lines or bacteria and mycoplasma which can alter the results. Regarding the mycoplasma contamination, tests to detect its presence in the cell medium are done every time a new cell line is thawed. Additionally, the cell lines are always manipulated in a Biosafety Level 2 containment environment to avoid cell contamination. Thus, in the future, we will also use primary pDCs to confirm our results and conclusions.

4.2. Conclusion

In conclusion, the data presented here indicate that proteasome inhibition induces an inflammatory response in pDCs in a cell specific manner, in the form of IL-1β secretion and cell death. The IL-1β secretion observed upon proteasome inhibition is independent of NLRP3-inflammasome activation. Furthermore, the lack of pyroptosis upon proteasome inhibition indicates that caspase-1 is not being activated. Together, these results suggest that the IL-1β secretion observed upon proteasome inhibition originates from a non-canonical pathway for IL-1β production. Regarding protein aggregation, this study shows that proteasome inhibition induces p62-based aggregates in pDCs, that are not essential for proteasome inhibition-mediated cell death. Based on these results, we propose further experimental work for the elucidation of the mechanisms by which proteasome inhibition induces inflammatory response on pDCs, and, also, to elucidate the role of p62 in that same inflammatory response.

Currently, accumulating preclinical evidence indicates that proteasome inhibitors are strong candidates for the treatment of immune-mediated disorder, including pDC derived immune-mediated disorders, such as systemic lupus erythematosus (75,77,78,80,96). However, our study could bring a new perspective into the use of proteasome inhibitors as drugs used to alleviate pDCs derived immune-mediated disorders. For the first time, we revealed that pDCs react to proteasome inhibition with a peculiar form of inflammatory response. This specific reaction could lead to exacerbation, instead of the desired alleviation, of the symptoms of an immune-mediated disorder, expected when a proteasome inhibitor is used as treatment for a pDCs derived immune-mediated disorders. Thus, other studies must be done in order to understand the real impact of proteasome inhibition on the immune system, with special focus on pDCs.

5. References

1. Chaplin DD. Overview of the immune response. J Allergy Clin Immunol. 2010 Feb;125(2):S3–23. Available from: https://linkinghub.elsevier.com/retrieve/pii/S0091674909028371
2. Martinon F, Aksentijevich I. New players driving inflammation in monogenic autoinflammatory diseases. Nat Rev Rheumatol. 2015 Jan 23;11(1):11–20. Available from: http://dx.doi.org/10.1038/nrrheum.2014.158
3. Agyemang AF, Harrison SR, Siegel RM, McDermott MF. Protein misfolding and dysregulated protein homeostasis in autoinflammatory diseases and beyond. Semin Immunopathol. 2015 Jul 21;37(4):335–47. Available from: http://link.springer.com/10.1007/s00281-015-0496-2
4. Shin JN, Fattah EA, Bhattacharya A, Ko S, Eissa NT. Inflammasome Activation by Altered Proteostasis. J Biol Chem. 2013 Dec 13;288(50):35886–95. Available from: http://www.jbc.org/lookup/doi/10.1074/jbc.M113.514919
5. Schraml BU, Reis e Sousa C. Defining dendritic cells. Curr Opin Immunol. 2015 Feb;32:13–20. Available from: http://dx.doi.org/10.1016/j.coi.2014.11.001
6. Mellman I, Steinman RM. Dendritic Cells. Cell. 2001 Aug;106(3):255–8. Available from: https://linkinghub.elsevier.com/retrieve/pii/S0092867401004494
7. Banchereau J, Steinman RM. Dendritic cells and the control of immunity. Nature. 1998 Mar 19;392(6673):245–52. Available from: http://dx.doi.org/10.1038/32588
8. Argüello RJ, Reverendo M, Gatti E, Pierre P. Regulation of protein synthesis and autophagy in activated dendritic cells: implications for antigen processing and presentation. Immunol Rev. 2016 Jul;272(1):28–38. Available from: http://doi.wiley.com/10.1111/imr.12427
9. Grouard G, Rissoan M-C, Filgueira L, Durand I, Banchereau J, Liu Y-J. The Enigmatic Plasmacytoid T Cells Develop into Dendritic Cells with Interleukin (IL)-3 and CD40-Ligand. J Exp Med. 1997 Mar 17;185(6):1101–12. Available from: http://www.jem.org/lookup/doi/10.1084/jem.185.6.1101
10. O'Doherty U, Peng M, Gezelter S, Swiggard WJ, Betjes M, Bhardwaj N, et al. Human blood contains two subsets of dendritic cells, one immunologically mature and the other immature. Immunology. 1994 Jul;82(3):487–93. Available from: http://www.ncbi.nlm.nih.gov/pubmed/7525461
11. Gilliet M, Cao W, Liu Y-J. Plasmacytoid dendritic cells: sensing nucleic acids in viral infection and autoimmune diseases. Nat Rev Immunol. 2008 Aug;8(8):594–606. Available from: http://www.nature.com/doifinder/10.1038/nri2358
12. Sozzani S, Vermi W, Del Prete A, Facchetti F. Trafficking properties of plasmacytoid dendritic cells in health and disease. Trends Immunol. 2010 Jul;31(7):270–7. Available from: http://dx.doi.org/10.1016/j.it.2010.05.004
13. Young LJ, Wilson NS, Schnorrer P, Proietto A, ten Broeke T, Matsuki Y, et al. Differential MHC class II synthesis and ubiquitination confers distinct antigen-presenting properties on conventional and plasmacytoid dendritic cells. Nat Immunol.

2008 Nov 12;9(11):1244–52. Available from: http://www.nature.com/articles/ni.1665

14. Jego G, Palucka AK, Blanck J-P, Chalouni C, Pascual V, Banchereau J. Plasmacytoid Dendritic Cells Induce Plasma Cell Differentiation through Type I Interferon and Interleukin 6. Immunity. 2003 Aug;19(2):225–34. Available from: http://www.ncbi.nlm.nih.gov/pubmed/12932356

15. Megjugorac NJ, Young HA, Amrute SB, Olshalsky SL, Fitzgerald-Bocarsly P. Virally stimulated plasmacytoid dendritic cells produce chemokines and induce migration of T and NK cells. J Leukoc Biol. 2004 Mar;75(3):504–14. Available from: http://doi.wiley.com/10.1189/jlb.0603291

16. Liu Y-J. IPC: Professional Type 1 Interferon-Producing Cells and Plasmacytoid Dendritic Cell Precursors. Annu Rev Immunol. 2005 Apr;23(1):275–306. Available from: http://www.annualreviews.org/doi/10.1146/annurev.immunol.23.021704.115633

17. Villadangos JA, Young L. Antigen-Presentation Properties of Plasmacytoid Dendritic Cells. Immunity. 2008 Sep;29(3):352–61. Available from: https://linkinghub.elsevier.com/retrieve/pii/S1074761308003816

18. Lelouard H, Gatti E, Cappello F, Gresser O, Camosseto V, Pierre P. Transient aggregation of ubiquitinated proteins during dendritic cell maturation. Nature. 2002 May;417(6885):177–82. Available from: http://www.nature.com/articles/417177a

19. DeFillopo A, Dai J, Li Z. Heat shock-induced dendritic cell maturation is coupled by transient aggregation of ubiquitinated proteins independently of heat shock factor 1 or inducible heat shock protein 70. Mol Immunol. 2004 Jul;41(8):785–92. Available from: https://linkinghub.elsevier.com/retrieve/pii/S0161589004001051

20. Kopito RR. Aggresomes, inclusion bodies and protein aggregation. Trends Cell Biol. 2000 Dec;10(12):524–30. Available from: https://linkinghub.elsevier.com/retrieve/pii/S0962892400018523

21. Canadien V, Tan T, Zilber R, Szeto J, Perrin AJ, Brumell JH. Cutting Edge: Microbial Products Elicit Formation of Dendritic Cell Aggresome-Like Induced Structures in Macrophages. J Immunol. 2005 Mar 1;174(5):2471–5. Available from: http://www.jimmunol.org/cgi/doi/10.4049/jimmunol.174.5.2471

22. Lelouard H, Schmidt EK, Camosseto V, Clavarino G, Ceppi M, Hsu H-T, et al. Regulation of translation is required for dendritic cell function and survival during activation. J Cell Biol. 2007 Dec 31;179(7):1427–39. Available from: http://www.jcb.org/lookup/doi/10.1083/jcb.200707166

23. Lelouard H, Ferrand V, Marguet D, Bania J, Camosseto V, David A, et al. Dendritic cell aggresome-like induced structures are dedicated areas for ubiquitination and storage of newly synthesized defective proteins. J Cell Biol. 2004 Mar 1;164(5):667–75. Available from: http://www.jcb.org/lookup/doi/10.1083/jcb.200312073

24. Hershko A, Ciechanover A. The ubiquitin system. Annu Rev Biochem. 1998 Jun 1;67(1):425–79. Available from: https://doi.org/10.1146/annurev.biochem.67.1.425

25. Thrower JS, Hoffman L, Rechsteiner M, Pickart CM. Recognition of the polyubiquitin proteolytic signal. EMBO J. 2000 Jan 4;19(1):94–102. Available from: http://www.ncbi.nlm.nih.gov/pmc/articles/PMC1171781/

26. Pierre P. Dendritic cells, DRiPs, and DALIS in the control of antigen processing.

Immunol Rev. 2005 Oct;207(1):184–90. Available from: http://doi.wiley.com/10.1111/j.0105-2896.2005.00300.x

27. Yewdell JW, Schubert U, Bennink JR. At the crossroads of cell biology and immunology: DRiPs and other sources of peptide ligands for MHC class I molecules. J Cell Sci. 2001 Mar;114(Pt 5):845–51. Available from: http://www.ncbi.nlm.nih.gov/pubmed/11181168

28. Reits EAJ, Vos JC, Grommé M, Neefjes J. The major substrates for TAP in vivo are derived from newly synthesized proteins. Nature. 2000 Apr 13;404(6779):774–8. Available from: http://dx.doi.org/10.1038/35008103

29. Wenger T, Terawaki S, Camosseto V, Abdelrassoul R, Mies A, Catalan N, et al. Autophagy inhibition promotes defective neosynthesized proteins storage in ALIS, and induces redirection toward proteasome processing and MHCI-restricted presentation. Autophagy. 2012 Mar 19;8(3):350–63. Available from: http://www.tandfonline.com/doi/abs/10.4161/auto.18806

30. Herter S, Osterloh P, Hilf N, Rechtsteiner G, Höhfeld J, Rammensee H-G, et al. Dendritic Cell Aggresome-Like-Induced Structure Formation and Delayed Antigen Presentation Coincide in Influenza Virus-Infected Dendritic Cells. J Immunol. 2005 Jul 15;175(2):891–8. Available from: http://www.jimmunol.org/cgi/doi/10.4049/jimmunol.175.2.891

31. Terawaki S, Camosseto V, Prete F, Wenger T, Papadopoulos A, Rondeau C, et al. RUN and FYVE domain–containing protein 4 enhances autophagy and lysosome tethering in response to Interleukin-4. J Cell Biol. 2015 Sep 28;210(7):1133–52. Available from: http://www.jcb.org/lookup/doi/10.1083/jcb.201501059

32. Montagna D, Sommi P, Necchi V, Vitali A, Montini E, Turin I, et al. Different Polyubiquitinated Bodies in Human Dendritic Cells: IL-4 Causes PaCS During Differentiation while LPS or IFNα Induces DALIS During Maturation. Sci Rep. 2017 Dec 12;7(1):1844. Available from: http://dx.doi.org/10.1038/s41598-017-02090-8

33. Szeto J, Kaniuk NA, Canadien V, Nisman R, Mizushima N, Yoshimori T, et al. ALIS are Stress-Induced Protein Storage Compartments for Substrates of the Proteasome and Autophagy. Autophagy. 2006 Jul 22;2(3):189–99. Available from: http://www.tandfonline.com/doi/abs/10.4161/auto.2731

34. Mizushima N, Yoshimori T, Ohsumi Y. The Role of Atg Proteins in Autophagosome Formation. Annu Rev Cell Dev Biol. 2011 Nov 10;27(1):107–32. Available from: https://doi.org/10.1146/annurev-cellbio-092910-154005

35. Takahama M, Akira S, Saitoh T. Autophagy limits activation of the inflammasomes. Immunol Rev. 2018 Jan;281(1):62–73. Available from: http://doi.wiley.com/10.1111/imr.12613

36. Lamark T, Johansen T. Aggrephagy: Selective Disposal of Protein Aggregates by Macroautophagy. Int J Cell Biol. 2012;2012:1–21. Available from: http://www.hindawi.com/journals/ijcb/2012/736905/

37. Into T, Inomata M, Niida S, Murakami Y, Shibata K. Regulation of MyD88 Aggregation and the MyD88-dependent Signaling Pathway by Sequestosome 1 and Histone Deacetylase 6. J Biol Chem. 2010 Nov 12;285(46):35759–69. Available from: http://www.jbc.org/lookup/doi/10.1074/jbc.M110.126904

38. Valečka J, Almeida CR, Su B, Pierre P, Gatti E. Autophagy and MHC-restricted

antigen presentation. Mol Immunol. 2018 Jul;99(May):163–70. Available from: https://linkinghub.elsevier.com/retrieve/pii/S0161589018301548

39. Münz C. Enhancing Immunity Through Autophagy. Annu Rev Immunol. 2009 Apr;27(1):423–49. Available from: http://www.annualreviews.org/doi/10.1146/annurev.immunol.021908.132537

40. Dengjel J, Schoor O, Fischer R, Reich M, Kraus M, Muller M, et al. Autophagy promotes MHC class II presentation of peptides from intracellular source proteins. Proc Natl Acad Sci. 2005 May 31;102(22):7922–7. Available from: http://www.pnas.org/cgi/doi/10.1073/pnas.0501190102

41. Blum JS, Wearsch PA, Cresswell P. Pathways of Antigen Processing. Annu Rev Immunol. 2013 Mar 21;31(1):443–73. Available from: http://www.annualreviews.org/doi/10.1146/annurev-immunol-032712-095910

42. Lee HK, Lund JM, Ramanathan B, Mizushima N, Iwasaki A. Autophagy-Dependent Viral Recognition by Plasmacytoid Dendritic Cells. Science (80-). 2007 Mar 9;315(5817):1398–401. Available from: http://www.sciencemag.org/cgi/doi/10.1126/science.1136880

43. Tal MC, Sasai M, Lee HK, Yordy B, Shadel GS, Iwasaki A. Absence of autophagy results in reactive oxygen species-dependent amplification of RLR signaling. Proc Natl Acad Sci. 2009 Feb 24;106(8):2770–5. Available from: http://www.pnas.org/cgi/doi/10.1073/pnas.0807694106

44. Jounai N, Takeshita F, Kobiyama K, Sawano A, Miyawaki A, Xin K-Q, et al. The Atg5 Atg12 conjugate associates with innate antiviral immune responses. Proc Natl Acad Sci. 2007 Aug 28;104(35):14050–5. Available from: http://www.pubmedcentral.nih.gov/articlerender.fcgi?artid=1955809&tool=pmcentrez&rendertype=abstract

45. Saitoh T, Fujita N, Hayashi T, Takahara K, Satoh T, Lee H, et al. Atg9a controls dsDNA-driven dynamic translocation of STING and the innate immune response. Proc Natl Acad Sci. 2009 Dec 8;106(49):20842–6. Available from: http://www.pnas.org/cgi/doi/10.1073/pnas.0911267106

46. Moscat J, Diaz-Meco MT. p62 at the Crossroads of Autophagy, Apoptosis, and Cancer. Cell. 2009 Jun;137(6):1001–4. Available from: https://linkinghub.elsevier.com/retrieve/pii/S0092867409006199

47. Rouschop KMA, Ramaekers CHMA, Schaaf MBE, Keulers TGH, Savelkouls KGM, Lambin P, et al. Autophagy is required during cycling hypoxia to lower production of reactive oxygen species. Radiother Oncol. 2009 Sep;92(3):411–6. Available from: http://dx.doi.org/10.1016/j.radonc.2009.06.029

48. Deretic V, Saitoh T, Akira S. Autophagy in infection, inflammation and immunity. Nat Rev Immunol. 2013 Oct 25;13(10):722–37. Available from: http://dx.doi.org/10.1038/nri3532

49. Levine B, Mizushima N, Virgin HW. Autophagy in immunity and inflammation. Nature. 2011 Jan 20;469(7330):323–35. Available from: http://www.nature.com/articles/nature09782

50. Saitoh T, Fujita N, Jang MH, Uematsu S, Yang B-G, Satoh T, et al. Loss of the autophagy protein Atg16L1 enhances endotoxin-induced IL-1β production. Nature. 2008 Nov 5;456(7219):264–8. Available from:

http://www.nature.com/articles/nature07383

51. Zhou R, Yazdi AS, Menu P, Tschopp J. A role for mitochondria in NLRP3 inflammasome activation. Nature. 2011 Jan 1;469(7329):221–5. Available from: http://www.nature.com/articles/nature09663

52. Dupont N, Jiang S, Pilli M, Ornatowski W, Bhattacharya D, Deretic V. Autophagy-based unconventional secretory pathway for extracellular delivery of IL-1β. EMBO J. 2011 Nov 30;30(23):4701–11. Available from: http://dx.doi.org/10.1038/emboj.2011.398

53. Shi C, Shenderov K, Huang N, Kabat J, Abu-Asab M, Fitzgerald KA, et al. Activation of autophagy by inflammatory signals limits IL-1β production by targeting ubiquitinated inflammasomes for destruction. Nat Immunol. 2012 Mar 29;13(3):255–63. Available from: http://www.nature.com/articles/ni.2215

54. Schroder K, Tschopp J. The Inflammasomes. Cell. 2010 Mar;140(6):821–32. Available from: https://linkinghub.elsevier.com/retrieve/pii/S0092867410000759

55. Miao EA, Rajan J V., Aderem A. Caspase-1-induced pyroptotic cell death. Immunol Rev. 2011 Sep;243(1):206–14. Available from: http://doi.wiley.com/10.1111/j.1600-065X.2011.01044.x

56. Youm Y, Grant RW, Mccabe LR, Albarado DC, Yen K, Ravussin A, et al. Canonical Nlrp3 inflammasome links systemic low grade inflammation to functional decline in aging. 2014;18(4):519–32.

57. Yang Y, Wang H, Kouadir M, Song H, Shi F. Recent advances in the mechanisms of NLRP3 inflammasome activation and its inhibitors. Cell Death Dis. 2019 Feb 12;10(2):128. Available from: http://dx.doi.org/10.1038/s41419-019-1413-8

58. Guarda G, Zenger M, Yazdi AS, Schroder K, Ferrero I, Menu P, et al. Differential Expression of NLRP3 among Hematopoietic Cells. J Immunol. 2011 Feb 15;186(4):2529–34. Available from: http://www.jimmunol.org/lookup/doi/10.4049/jimmunol.1002720

59. Cruz MT, Ferreira I, Liberal J, D Martins J, Silva A, Neves BM. Inflammasome in Dendritic Cells Immunobiology: Implications to Diseases and Therapeutic Strategies. Curr Drug Targets. 2017 Jun 2;18(9):1003–18. Available from: http://www.eurekaselect.com/145693/article

60. Yu X, Du Y, Cai C, Cai B, Zhu M, Xing C, et al. Inflammasome activation negatively regulates MyD88-IRF7 type I IFN signaling and anti-malaria immunity. Nat Commun. 2018 Dec 23;9(1):4964. Available from: http://dx.doi.org/10.1038/s41467-018-07384-7

61. Cromm PM, Crews CM. The Proteasome in Modern Drug Discovery: Second Life of a Highly Valuable Drug Target. ACS Cent Sci. 2017 Aug 23;3(8):830–8. Available from: http://pubs.acs.org/doi/10.1021/acscentsci.7b00252

62. Varshavsky A. Regulated protein degradation. Trends Biochem Sci. 2005 Jun;30(6):283–6. Available from: https://linkinghub.elsevier.com/retrieve/pii/S0968000405000952

63. Tanaka K. The proteasome: Overview of structure and functions. Proc Japan Acad Ser B. 2009;85(1):12–36. Available from: http://joi.jlc.jst.go.jp/JST.JSTAGE/pjab/85.12?from=CrossRef

64. Komander D, Rape M. The Ubiquitin Code. Annu Rev Biochem. 2012 Jul 7;81(1):203–29. Available from: http://www.annualreviews.org/doi/10.1146/annurev-biochem-060310-170328

65. Kisselev AF, Goldberg AL. Proteasome inhibitors: from research tools to drug candidates. Chem Biol. 2001;8(8):739–58. Available from: https://linkinghub.elsevier.com/retrieve/pii/S1074552101000564

66. Wenzel T, Baumeister W. Conformational constraints in protein degradation by the 20S proteasome. Nat Struct Mol Biol. 1995 Mar 1;2(3):199–204. Available from: https://doi.org/10.1038/nsb0395-199

67. Budenholzer L, Cheng CL, Li Y, Hochstrasser M. Proteasome Structure and Assembly. J Mol Biol. 2017 Nov;429(22):3500–24. Available from: https://linkinghub.elsevier.com/retrieve/pii/S002228361730270X

68. Murata S, Sasaki K, Kishimoto T, Niwa S -i., Hayashi H, Takahama Y, et al. Regulation of CD8+ T Cell Development by Thymus-Specific Proteasomes. Science (80-). 2007 Jun 1;316(5829):1349–53. Available from: http://www.sciencemag.org/cgi/doi/10.1126/science.1141915

69. Murata S, Takahama Y, Tanaka K. Thymoproteasome: probable role in generating positively selecting peptides. Curr Opin Immunol. 2008 Apr;20(2):192–6. Available from: https://linkinghub.elsevier.com/retrieve/pii/S0952791508000265

70. Basler M, Kirk CJ, Groettrup M. The immunoproteasome in antigen processing and other immunological functions. Curr Opin Immunol. 2013 Feb;25(1):74–80. Available from: http://dx.doi.org/10.1016/j.coi.2012.11.004

71. Konstantinova IM, Tsimokha AS, Mittenberg AG. Role of Proteasomes in Cellular Regulation. In: International Review of Cell and Molecular Biology. 2008. p. 59–124. Available from: https://linkinghub.elsevier.com/retrieve/pii/S1937644808006023

72. Schmidt M, Finley D. Regulation of proteasome activity in health and disease. Biochim Biophys Acta - Mol Cell Res. 2014 Jan;1843(1):13–25. Available from: https://linkinghub.elsevier.com/retrieve/pii/S0167488913003108

73. Hoeller D, Dikic I. Targeting the ubiquitin system in cancer therapy. Nature. 2009 Mar 25;458(7237):438–44. Available from: http://www.nature.com/articles/nature07960

74. Kaur G, Batra S. Emerging role of immunoproteasomes in pathophysiology. Immunol Cell Biol. 2016 Oct;94(9):812–20. Available from: http://doi.wiley.com/10.1038/icb.2016.50

75. Nencioni A, Garuti A, Schwarzenberg K, Cirmena G, Dal Bello G, Rocco I, et al. Proteasome inhibitor-induced apoptosis in human monocyte-derived dendritic cells. Eur J Immunol. 2006 Mar;36(3):681–9. Available from: http://doi.wiley.com/10.1002/eji.200535298

76. Blanco B, Sánchez-Abarca LI, Caballero-Velázquez T, Santamaría C, Inogés S, Pérez-Simón JA. Depletion of alloreactive T-cells in vitro using the proteasome inhibitor bortezomib preserves the immune response against pathogens. Leuk Res. 2011 Oct;35(10):1412–5. Available from: https://linkinghub.elsevier.com/retrieve/pii/S0145212611002517

77. Nencioni A, Schwarzenberg K, Brauer KM, Schmidt SM, Ballestrero A, Grünebach F, et al. Proteasome inhibitor bortezomib modulates TLR4-induced dendritic cell

activation. Blood. 2006 Jul 15;108(2):551–8. Available from: http://www.bloodjournal.org/cgi/doi/10.1182/blood-2005-08-3494

78. Straube C, Wehner R, Wendisch M, Bornhäuser M, Bachmann M, Rieber EP, et al. Bortezomib significantly impairs the immunostimulatory capacity of human myeloid blood dendritic cells. Leukemia. 2007 Jul 10;21(7):1464–71. Available from: http://www.nature.com/articles/2404734

79. Subklewe M, Sebelin-Wulf K, Beier C, Lietz A, Mathas S, Dörken B, et al. Dendritic Cell Maturation Stage Determines Susceptibility to the Proteasome Inhibitor Bortezomib. Hum Immunol. 2007 Mar;68(3):147–55. Available from: https://linkinghub.elsevier.com/retrieve/pii/S0198885906006124

80. Hirai M, Kadowaki N, Kitawaki T, Fujita H, Takaori-Kondo A, Fukui R, et al. Bortezomib suppresses function and survival of plasmacytoid dendritic cells by targeting intracellular trafficking of Toll-like receptors and endoplasmic reticulum homeostasis. Blood. 2011 Jan 13;117(2):500–9. Available from: https://ashpublications.org/blood/article/117/2/500/28149/Bortezomib-suppresses-function-and-survival-of

81. Ainscough JS, Frank Gerberick G, Zahedi-Nejad M, Lopez-Castejon G, Brough D, Kimber I, et al. Dendritic Cell IL-1α and IL-1β Are Polyubiquitinated and Degraded by the Proteasome. J Biol Chem. 2014 Dec 19;289(51):35582–92. Available from: http://www.jbc.org/lookup/doi/10.1074/jbc.M114.595686

82. Liang Y, Ma S, Zhang Y, Wang Y, Cheng Q, Wu Y, et al. IL-1β and TLR4 Signaling Are Involved in the Aggravated Murine Acute Graft-versus-Host Disease Caused by Delayed Bortezomib Administration. J Immunol. 2014 Feb 1;192(3):1277–85. Available from: http://www.jimmunol.org/lookup/doi/10.4049/jimmunol.1203428

83. Karlsson AB, Washington J, Dimitrova V, Hooper C, Shekhtman A, Bakowska JC. The role of spartin and its novel ubiquitin binding region in DALIS occurrence. Lemmon S, editor. Mol Biol Cell. 2014 Apr 15;25(8):1355–65. Available from: https://www.molbiolcell.org/doi/10.1091/mbc.e13-11-0705

84. Mitchell D, Chintala S, Dey M. Plasmacytoid dendritic cell in immunity and cancer. J Neuroimmunol. 2018 Sep;322(February):63–73. Available from: https://doi.org/10.1016/j.jneuroim.2018.06.012

85. Swiecki M, Colonna M. The multifaceted biology of plasmacytoid dendritic cells. Nat Rev Immunol. 2015 Aug 10;15(8):471–85. Available from: http://dx.doi.org/10.1038/nri3865

86. Cong L, Ran FA, Cox D, Lin S, Barretto R, Habib N, et al. Multiplex genome engineering using CRISPR/Cas systems. Science. 2013 Feb 15;339(6121):819–23. Available from: http://www.sciencemag.org/cgi/doi/10.1126/science.1231143

87. Tanida I, Ueno T, Kominami E. LC3 conjugation system in mammalian autophagy. Int J Biochem Cell Biol. 2004 Dec;36(12):2503–18. Available from: https://linkinghub.elsevier.com/retrieve/pii/S1357272504002110

88. Kirkin V, Lamark T, Sou Y-S, Bjørkøy G, Nunn JL, Bruun J-A, et al. A Role for NBR1 in Autophagosomal Degradation of Ubiquitinated Substrates. Mol Cell. 2009 Feb;33(4):505–16. Available from: https://linkinghub.elsevier.com/retrieve/pii/S1097276509000641

89. Bergsbaken T, Fink SL, Cookson BT. Pyroptosis: host cell death and inflammation.

Nat Rev Microbiol. 2009 Feb;7(2):99–109. Available from: http://www.nature.com/articles/nrmicro2070

90. MG-132 - CAS 133407-82-6 - Calbiochem CAS 133407-82-6 | 474790. [cited 2019 Oct 7]. Available from: http://www.merckmillipore.com/PT/en/product/MG-132-CAS-133407-82-6-Calbiochem,EMD_BIO-474790?RedirectedFrom=http%253A%252F%252Fwww.merck-chemicals.com%252Fgermany%252Flife-science-research%252Fmg-132%252FEMD_BIO-474790%252Fp_w_.b.s1LzxMAAAEW02EfVhTm&ReferrerURL=https%253A%25

91. de Zoete MR, Palm NW, Zhu S, Flavell RA. Inflammasomes. Cold Spring Harb Perspect Biol. 2014 Dec 1;6(12):a016287–a016287. Available from: http://cshperspectives.cshlp.org/lookup/doi/10.1101/cshperspect.a016287

92. Feltham R, Vince JE, Lawlor KE. Caspase-8: not so silently deadly. Clin Transl Immunol. 2017 Jan 6;6(1):e124. Available from: http://dx.doi.org/10.1038/cti.2016.83

93. Moriwaki K, Bertin J, Gough PJ, Chan FK-M. A RIPK3–Caspase 8 Complex Mediates Atypical Pro–IL-1β Processing. J Immunol. 2015 Feb 15;194(4):1938–44. Available from: http://www.jimmunol.org/lookup/doi/10.4049/jimmunol.1402167

94. Sánchez-Martín P, Komatsu M. p62/SQSTM1 – steering the cell through health and disease. J Cell Sci. 2018 Nov 1;131(21):jcs222836. Available from: http://jcs.biologists.org/lookup/doi/10.1242/jcs.222836

95. Liu WJ, Ye L, Huang WF, Guo LJ, Xu ZG, Wu HL, et al. p62 links the autophagy pathway and the ubiqutin–proteasome system upon ubiquitinated protein degradation. Cell Mol Biol Lett. 2016 Dec 13;21(1):29. Available from: http://dx.doi.org/10.1186/s11658-016-0031-z

96. Ichikawa HT, Conley T, Muchamuel T, Jiang J, Lee S, Owen T, et al. Beneficial effect of novel proteasome inhibitors in murine lupus via dual inhibition of type I interferon and autoantibody-secreting cells. Arthritis Rheum. 2012 Feb;64(2):493–503. Available from: http://www.ncbi.nlm.nih.gov/pubmed/21905015

6. Annexes

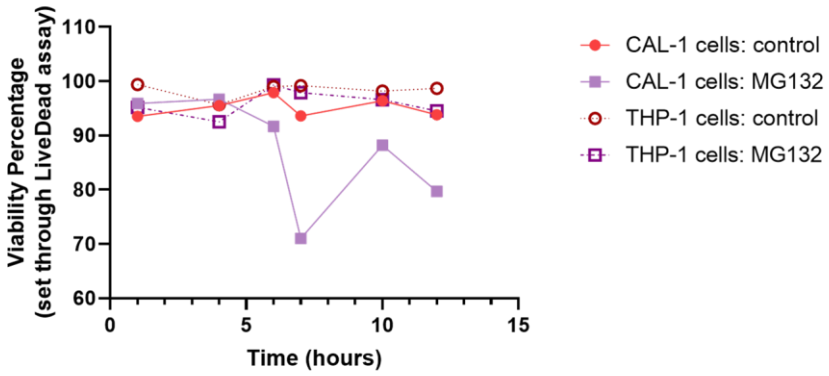

Supplemental Figure 1: Evaluation of cell viability through flow cytometry analyses. The LIVE/DEAD™ Fixable Far-Red Dead Cell Stain Kit (Invitrogen, L34973) was used to determine the viability of CAL-1 and THP-1 cells. CAL-1 and THP-1 were treated with 10 µM of MG132. Cell viability was evaluated after 1, 4, 6, 7, 10 and 12 hours of incubation. (Data kindly provided by Daniela Barros)

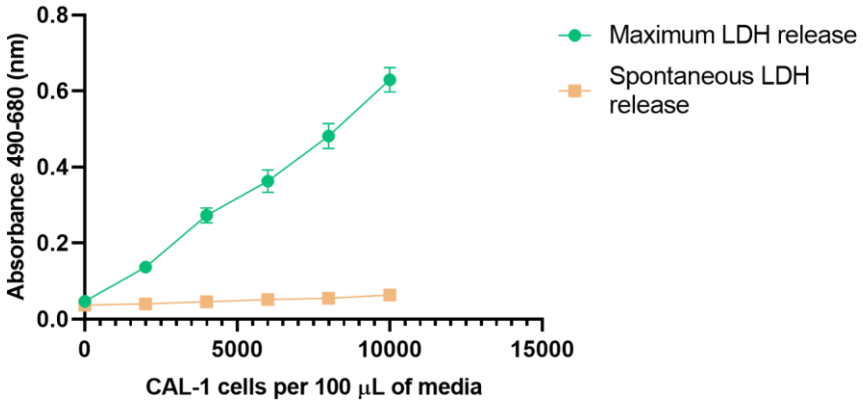

Supplemental Figure 2: Determination of the optimum CAL-1 cell number for LDH cytotoxicity assay. A supernatants were collected after optimization procedure and used for measurement of Maximum LDH realease in media and Spontaneous LDH release in media by cyQUANT™ LDH Cytotoxicity Assay Kit as described in methods.

Supplemental Table 1: Variation of IL-1β concentration in CAL-1 cells throughout the study

IL-1β Concentration (pg/ml)

CAL-1 cells

Date	Control	MG132	Spautin-1
13.03.19	12,66667	61,167	0
10.04.19	0	16,15386	26,61539
24.06.19	0	25,088	14,614
18.06.19	0	5,035	-
4.07.19	3,179	6,218	0,000
24.07.19	0	25,088	14,614
30.07.19	19,255	0	13,78
8.8.19	40,784	16,196	36,902
18.9.19	35,862	39,362	39,612
22.09.19	46,162	45,912	46,962
01.10.19	33,612	21,562	19,762